

**Alberta front ranges lidar snow depth assessment:
Final report**

Submitted to:

John Diiwu, Ph.D., Sustainable Resources Development, Government of Alberta

&

Edith Philips, Regulatory Affairs, City of Calgary

by:

Chris Hopkinson, Ph.D.

Research Scientist,

Applied Geomatics Research Group, Middleton, NS

Email: chris.hopkinson@nsc.ca

&

Tim Collins

Acadia University, Wolfville, NS

February 15th, 2009



Table of Contents

Table of Contents.....	2
Tables and Figures	3
Summary.....	5
Introduction.....	7
Objectives	7
Rationale.....	7
Background	8
Airborne LiDAR	8
Controls on Snowpack distribution	10
Study Area.....	11
Methods.....	14
Data Collection	14
LiDAR Processing and Snow Surface DEM Generation.....	18
Analysis of Field and LiDAR Data	19
Terrascan	19
Golden Software Surfer	21
Arcmap.....	22
Creation of the Elbow Watershed	27
Snow water Equivalent field data results.....	30
Marmot Creek area field & LiDAR snowpack depth distribution observations	31
Elbow watershed field and lidar snowpack depth distribution observations	34
Elevation:	35
Slope:	36
Aspect:	38
Canopy Cover:.....	39
Regional or west to east gradient effects:.....	40

Elbow Watershed LiDAR-based snow volume estimation	41
Average snow depth method	41
Average snow depth by watershed attributes	42
GIS Model	44
Discussion and Conclusions	48
Acknowledgements	52
LiDAR and snowpack bibliography:.....	54
Appendices	59
A.1. Individual Transect Summaries	59
A.2. AVI Crown Closure comparison to DHP canopy fractional cover	62

Tables and Figures

Figure 1: Study area location and airborne LiDAR survey transects over Elbow and Marmot survey polygon. Field sampling locations are illustrated as green markers.....	13
Figure 2. Proposed field and airborne data collection plan.	15
Figure 3. Field snow depth sampling designs.....	16
Figure 4: Example of horizontal shift over building roof between summer and winter datasets.....	20
Figure 5: Example of Elbow Creek area LiDAR elevation dataset classed into 100m bins.....	23
Figure 6. Elevation hypsometry of Marmot study area.....	24
Figure 7. Marmot area digital elevation model.....	24
Figure 8. Marmot area aspect and slope maps.	25
Figure 9. TWI and Terrain morphology.....	26
Figure 10. Canopy Fractional Cover (FC) and winter radiation load over Marmot Creek area.	27
Figure 11: Elbow River watershed classified by elevation.....	28
Table 1. Snow Water Equivalent sampling results from Elbow Watershed.Marmot Creek area field & LiDAR snowpack depth distribution observations	30
Figure 12. Spatial variation of snow depth over the Marmot creek and Nakiska ski hill area. Note deeper snow evident in tree lined ski runs at south end of image.....	31
Figure 13. Marmot area snow depth stratification by terrain and landcover attribute.	32

Table 2. Summary statistics of snow depth by terrain and landcover attribute.	32
Table 3. Snow depth with elevation	33
Figure 14. Snow depth with elevation and terrain.	33
Figure 15. Mean field snow depth stratified by elevation	35
Figure 16. Mean LiDAR snow depth stratified by elevation.	35
Figure 17. Mean field snow depth stratified by slope angle	36
Figure 18. Mean LiDAR snow depth stratified by elevation.	36
Figure 19. Mean field snow depth stratified by aspect	38
Figure 20. Mean LiDAR snow depth stratified by aspect.....	38
Figure 21. Mean field snow depth stratified by canopy cover.	39
Figure 22. Mean field snow depth stratified by elevation	39
Figure 23. West to east gradient in LiDAR-based snow depth.	40
Table 4. Snow water equivalent estimation for the Elbow River watershed	42
Table 5. Snow water equivalent estimation for the Elbow River watershed	43
Table 6. Mean snow depth for reclassified GIS model	44
Table 7. Snow water equivalent calculated by re-classed GIS model	46
Figure 24. LiDAR-based GIS snow depth model applied to Elbow River watershed	47
Figure 25: Example of how slope affects vertical accuracy	49
Figure 26: Inter-relation of horizontal and vertical error due to slope	50

Summary

This report summarizes the LiDAR snowpack mapping proof of concept analysis conducted over the Marmot and Elbow Watersheds in Kananaskis Country and the foothills of the Canadian Rocky mountains. Hopkinson has carried out the Marmot analysis whilst Collins has conducted the Elbow analysis as part of his master's research under Hopkinson's direction. The Marmot analysis has focused more on establishing patterns of snowpack distribution and relating these patterns to specific terrain and land cover attributes. The Elbow analysis has focused more on testing a lidar snow depth sampling methodology, establishing some basic relationships and applying these to derive a watershed estimate of snowpack volume and snow water equivalent (SWE) in a GIS environment. To date, only the field data collected by the AGRG team have been compiled and so only field data related to Elbow are presented. The AGRG team does not have snow depth collected in the Marmot area by the U of S team.

The mean snow depth from the 1675 field measurements collected in the Elbow area equaled 0.28m with a standard deviation of 0.27m. The LiDAR transect-based sampling mean snow depth was 0.18m with a standard deviation of 1.6m but after filtering the data for depths exceeding 5cm (noise level), the average became 0.26m; much closer to the field estimates which were collected only in snow covered areas. The high standard deviation in the LiDAR data illustrates the effects both of uncertainty (error) in the data plus a wide range of snow depths throughout the study area.

Elbow watershed total SWE estimates range from $34.5 \times 10^6 \text{m}^3$ to $46.9 \times 10^6 \text{m}^3$. The highest estimates are based on a linear extrapolation of the observed elevation trend within the LiDAR data collected on the northern side of the Elbow Watershed. The actual watershed has a greater elevation range than sampled by the Elbow LiDAR dataset and so linear extrapolation of the LiDAR results may not be appropriate. Indeed, in the Marmot LiDAR observations (Figure 14), there was a clear peak in snowpack depth at tree line with depths leveling off or reducing above this elevation (approx 2200m a.s.l). Therefore, linearly extrapolating snowpack depth with height probably leads to an overestimate of snowpack volume. The modified class-based GIS model for Elbow snow volume accounts for the drop off in snow depth observed above tree line in the Marmot LiDAR data and generates a SWE estimate that lies near the middle of the range at $42.6 \times 10^6 \text{m}^3$.

The results of our analysis suggest that the LiDAR-based estimate of SWE for the Elbow watershed above Bragg Creek is $40 \times 10^6 \text{m}^3 \pm 10 \times 10^6 \text{m}^3$. However, due to the shallow snow depth, sparse coverage, and various system and terrain related measurement uncertainties, the true value may deviate significantly from this estimated range. At the time of the LiDAR and field data collections, snow conditions were abnormally depleted relative to most years and this greatly limited what could be achieved with this experiment. The observed snowpack depths at both study sites (particularly Elbow) were close to the practical detection limit given expected LiDAR DEM uncertainties. With observed average snow depths in Elbow below 30cm it is actually quite encouraging that the LiDAR estimates were close. More reliable results would no doubt be achieved if the snowpack were deeper

but without co-registered LiDAR and field data it is impossible to accurately determine what the lowest viable average snow depth would be. We are convinced that it is above the depths observed in this study, as in almost all cases, the standard deviation of depth uncertainty was close to the mean; i.e. 100% uncertainty! For a practical application of this method, the uncertainty would have to be reduced to an acceptable level. If 25% uncertainty limits are considered acceptable, then this implies that average watershed depths would need to approach 1m. In many years, such conditions probably do occur in the upper reaches of the Elbow and almost certainly for other watersheds further west.

A logistical setback for this study was our inability to perform direct comparisons of field to LiDAR snow depth data due to the LiDAR survey lines not following the planned flight paths. In order to perform a more thorough sensitivity analysis of this method, the experiment could be performed again over an area of deeper snowpack with absolutely co-located field and LiDAR data. More work is also needed to validate the watershed estimate of SWE. This could involve running a hydrological model on the Elbow Creek during spring runoff and comparing to the flow records to see if the antecedent snowpack conditions derived by LiDAR leads to an accurate simulation of runoff magnitude.

Introduction

Objectives

The study has tested the efficacy of a single short lidar acquisition once per year to map snow depth across Rocky Mountains Watersheds in the Front Ranges and along densely forested foothill areas. For this proof-of-concept the Elbow Watershed up stream of Bragg Creek and area surrounding Marmot Creek near Kananaskis Village have been studied.

The study can be broken into the following components:

- 1) Collection of multiple scanning lidar transects (~ 30 km length) across Elbow Watershed and continuous polygon over Marmot Creek to directly capture the gradients and distributions in snowpack depth within montane landcovers and alpine terrains. The aerial surveys were arranged to capture a variety of forest canopy cover and terrain conditions.
- 2) Partial ground validation of the lidar snow depth measurements were conducted over Elbow and Marmot. The results for Elbow only are presented in this report.
- 3) Elevational and land cover stratification was used to develop a spatially explicit GIS model of snow depth for the Elbow Watershed.

Rationale

In North America, forested mountain areas are often the headwaters of rivers that flow into arid prairie regions and, as such, snowpack data are essential for regional annual water resource predictions. For example, the Bow River in Alberta, Canada rises in the Rocky Mountains and flows eastward into heavily irrigated prairie lands. Each year, helicopter snow surveys are employed between four and six times during winter months to assess basin-wide snow water equivalent at approximately 12 sites (Alberta Environmental Protection, 2000). Assuming that this task requires two field technicians and approximately 2 ½ hours of helicopter time for each day of snow surveys, the annual cost of this task amounts to approximately US\$12,000 (details obtained from Dick Allison, Water Management Services, Lethbridge, Alberta in 2003). For the same price, a one-day commercial airborne LiDAR survey could be mobilized to collect data over approximately 12,000 acres (50 km²) (prices based a quote by Airborne One in 2004) or over much larger areas of several hundred sq kms if a sampling strategy were employed. Although a LiDAR data collection campaign has limited temporal coverage, it gains substantially in terms of spatial coverage and high density sampling. A clear limitation of this approach is that a 'no snow' digital elevation model (DEM) is required in order that snow depth might be calculated. However, with much of the Province of Alberta now covered with baseline LiDAR DEM data, this water resource management application may soon be viable. The purpose of this study is to evaluate the technical merit of such a snowpack monitoring methodology.

Background

Knowledge of spring snowpack conditions is essential for the prediction of water availability and flood peaks following the onset of melt. Evaluating snowpack conditions in mountainous and forested regions is particularly important, as the terrain and canopy covers influence accumulation and melt processes, and therefore have a marked effect on the downstream hydrograph (e.g. Elder *et al.*, 1998). Current ground-based snow depth measurements are manually intensive, limited in spatial extent and generally costly in remote areas. In addition, manually assessing snowpack depth distribution under forest canopies can be difficult due to heterogeneous ground and understory conditions (Adams and Barr, 1970). There is a strong justification, therefore, for investigating remote techniques of snowpack distribution measurement in such areas. Derksen *et al.* (2001) demonstrated that passive microwave technology is useful for estimation of snow water equivalent (SWE) in forest regions. However, such methods are unreliable for dense canopies, during snowmelt or in areas of high relief (Derksen *et al.*, 2001), and the spatial resolution is very low. As will be discussed below, airborne LiDAR has also proven itself capable of mapping snow depth in forested (Hopkinson *et al.* 2004) and mountainous environments (Deems *et al.* 2006) but questions remain as to its accuracy and operational efficacy for monitoring purposes in such environments.

In mountainous environments, snow depth is expected to increase with elevation due to the orographic effect (Pomeroy and Gray, 2005). A strong relationship between terrain slope and snow depth is not expected due to the impact of other variables such as wind distribution. However, increased snow depth at shallow slope angles and less accumulation at near vertical angles can be anticipated (Anderton *et al.*, 2005). In addition, more snow cover is expected on north facing slopes than on south facing slopes due to solar radiation-induced melt (Sicart *et al.*, 2006). Canopy fractional cover is also expected to influence snow accumulation such that open areas will provide larger estimates than areas of complete canopy coverage, due to lack of canopy interception (Pomeroy and Gray, 2005; Hedstrom and Pomeroy, 1998; Pomeroy *et al.*, 2002; López-Moreno and Latron, 2008).

Airborne LiDAR

Airborne LiDAR (also referred to as laser altimetry) combines: (i) knowledge of the speed of light; (ii) the location of the laser head in space; and (iii) the time from laser pulse transmission to reception; to determine a three-dimensional co-ordinate on the ground. Utilising standard scanning technology, laser pulses are swept left and right, perpendicular to the line of flight resulting in a “saw tooth” pattern of surveyed points on the ground. The resultant data can be used to create a high-resolution (sub-metre) digital terrain model of the ground surface. To ensure the data collected represent actual ground conditions, it is necessary to reference the laser head (from which the laser pulse is emitted) to known control points on the ground. This is achieved using differential GPS, whereby at least one survey grade GPS receiver and antenna is located over a known control point (generally within 50 km of the survey area) and another is located inside the aircraft. Through post processing of the aircraft GPS trajectory, the location of the laser head is continually fixed in

space. The quality of the final data product is largely related to the accuracy of the GPS trajectory. Further refinement of the trajectory and compensation for aircraft attitude variation (i.e. pitch, roll and yaw) is achieved by post processing data collected by an onboard inertial navigation system (INS). Current technology can collect multiple returns at pulse repetition frequencies (PRF) exceeding 100 kHz. The resultant laser spot spacing on the ground can be as low as 20 cm in both x and y directions, and the ground swath typically varies between 0 and 3000 m depending on flying altitude and scan angle. For more information see Gutelius (1998) and Baltsavias (1999).

Airborne LiDAR is becoming increasingly popular for a variety of biogeophysical applications: e.g. forest structure (St-Onge *et al.*, 2000; Means *et al.*, 2000; Lim *et al.*, 2001; Lim *et al.*, 2003); glaciology (Kennet and Eiken, 1997; Hopkinson *et al.*, 2001); alpine watershed attribute extraction (Hopkinson *et al.*, 2008a). The cost effectiveness of airborne LiDAR over traditional manually intensive field techniques for flood mapping and environmental change detection has been demonstrated by Holden (1998). Some LiDAR-based change detection and monitoring techniques thus far proven are: icesheet melt (Krabill *et al.*, 1995); snowpack depth mapping beneath forest canopies (Hopkinson *et al.*, 2004); glacier downwasting and volume loss in the Canadian Rockies (Hopkinson and Demuth, 2006); forest growth assessment (Hopkinson *et al.*, 2008b); and others ranging from shoreline degradation to hydro wire damage in remote regions (Flood and Gutelius, 1997). Clearly, then, airborne LiDAR is a useful tool for the assessment of subtle changes in the landscape. However, the question remains as to whether or not repeat surveys using existing LiDAR technology can be used to generate accurate maps of snow depth and volume in heterogeneous mountainous and forest covered terrain.

There have been relatively few studies on the use of LiDAR to map snowpack depth. Hopkinson *et al.* (2004) investigated the ability of LiDAR to map snow pack depth beneath deciduous and coniferous forest canopies. Deems *et al.* (2006) investigated using LiDAR data to produce the Fractal Distribution of Snow Depth. Both authors employed a similar approach in which a DEM subtraction of a summer or fall (no snow cover) dataset from a winter dataset was computed in order to arrive at a map of snow depth. The conclusions of Hopkinson *et al.* (2004) demonstrated that LiDAR can provide a relatively accurate snow depth prediction for shallow accumulations of approximately 20cm to 40cm provided the terrain was relatively flat and the understory not too dense. The work of Deems *et al.* (2006) suggested that LiDAR could be used to evaluate snowpack distributions in mountainous environments over a larger scale.

The current study builds on this previous work by:

- a) investigating the ability of LiDAR to map snow depth in the Alberta Front Ranges environment that is both forested and mountainous;
- b) testing a transect-based sampling approach that will increase the cost effectiveness of LiDAR for these type of monitoring application;
- c) developing a stratified land cover/terrain model of snow depth that can be applied in a GIS to estimate watershed level snow volume.

Controls on Snowpack distribution

There has been much research in the field of snow distribution processes (Anderton *et al.*, 2004; Hedstrom *et al.*, 1998; Lopez-Monerno and Laton, 2008; Pomeroy and Gray, 1995; Sicart *et al.*, 2006). Many terrain attributes and processes influence snowpack distribution. Each factor exerts a different influence on the prediction of snow depth. Factors that influence snow depth include wind distribution, sublimation, solar radiation melt, gravitational redistribution, elevation gradients, and canopy fractional cover. Four terrain and land cover attributes that influence snow depth explored in this study include elevation, slope, aspect, and canopy fractional cover. These four factors were chosen over other attributes due to their *a priori* known influences on snow accumulation and distribution processes and the relative ease with which these attributes can be extracted from DEMs and land cover maps.

Slope as an indicator of snow depth has been researched with mixed results. Pomeroy and Gray (1995) indicated in their text book *Snow Cover Accumulation and Management* that varying snow depths on slopes were due more to wind direction, wind speed, and temperature during snow redistribution than to direct snowfall on the slope. A snow distribution study performed in the Spanish Central Pyrenees used slope as a predictor of snow depth because it was reasoned that slope affects the stability of the snowpack (Anderton *et al.*, 2004). However, this same study indicated that little correlation existed between snow depth and slope gradient.

Snow depth is affected by solar radiation: with more exposure of snow to solar radiation, more melting will occur. Sicart *et al.*, (2006) explains how solar radiation affects the melt of the snowpack. As a simple predictor of solar radiation exposure, the slope aspect can be used to predict snowpack depths. The effects of aspect are most evident during periods of snow melt than accumulation (Pomeroy and Gray, 1995). Snow disappears first from the south-facing slopes since they receive the highest concentration of solar radiation. Anderton *et al.* (2004) used aspect as one of their snow depth predictors in research conducted in the Spanish Pyrenees. In this study the same catchment was monitored in two consecutive years (1997 and 1998). Results of this study indicated that in 1997 there was a strong relationship between aspect and resulting snow accumulation; however in 1998 the relationship was weak. Despite the weak relationship it was found that the areas of maximum snow melt were located on south facing slopes. However, aspect alone may not be a good indicator of snow depth because slopes that are shaded by topographic features such as larger mountain peaks or dense foliage will receive reduced sun exposure regardless of slope aspect.

Elevation is often positively correlated to snow depth accumulation: the higher the elevation the greater the snow accumulation. Pomeroy and Gray, (1995) describe that where vegetation, micro relief and other factors do not vary with elevation, snow depth usually increases with elevation. This is partly due to the increasing number of snowfall events and a decrease in evaporation and melt. Orographic precipitation enhances the amount of snowfall at higher elevation due to the rising of moist air across the mountain range. Anderton *et al.*, (2004) showed results that did not support a relationship between elevation and snow depth within their study area.

Canopy fractional cover has been shown to be a significant controlling factor in snow accumulation (Pomeroy and Gray, 2005; Hedstrom and Pomeroy, 1998; Pomeroy *et al.*, 2002; López-Moreno and Latron, 2008). As canopy coverage increases to 100%, the amount of snow accumulation decreases (Pomeroy and Gray, 2005). Snow accumulation decreases as a result of sublimation of the snow that has been intercepted by the tree limbs as well as the effects of snow falling from the limbs (i.e. snow distribution and density) (Pomeroy and Gray, 2005; Hedstrom and Pomeroy, 1998). Hedstrom and Pomeroy, (1998) determined that the interception efficiency increases with an increasing leaf area index (LAI) and canopy coverage. It has been shown that

clearings in the forest that are about 2 to 3 times as wide as the tree height have a greater snow accumulation than that of larger clearings because wind transport has a larger effect on snow distribution in the larger clearings (Essery *et al.*, 1999; López-Moreno and Latron, 2008; Pomeroy and Gray, 2005).

It has been found that greater snow depths are found in more sheltered locations (Anderton *et al.*, 2004). Other considerations related to wind are the height and quality of vegetation cover. In the event of wind blowing through tall trees the effect on snowpack transport will be minimal due to the blocking effect by the trees. Trees act as obstacles, decreasing the wind velocity substantially on their lee sides, effectively acting as snow fences and facilitating the accumulation of large quantities of snow (Heimstra *et al.* 2002; Pomeroy and Gray 1995). In clearings, shrubs act as friction cover and higher accumulation will occur than over flat featureless terrain (Essery *et al.*, 1999; Pomeroy and Gray, 1995). In clearings with little to no vegetation snow accumulation will be minimal due to wind transport (Essery *et al.*, 1999; Pomeroy and Gray, 1995). Above the tree line in the mountainous region snow accumulation will be minimal due to wind transport and sublimation. Pomeroy and Gray (1995) reported that 15 – 40% of snow sublimation that occurs on the Canadian Prairies occurs due to blowing snow sublimation.

Study Area

Two areas have been chosen as the focus of this study (Figure 1). Primarily, the Elbow River watershed, which is located to the west of Calgary, Alberta and secondarily, the Marmot Creek area further to the west in the high mountains of Kananaskis Country. Both watersheds drain into the Bow River but snow that melts and runs off from this Elbow is held in the Glenmore Reservoir for irrigation and drinking water. The Elbow provides a significant portion of the water that is used by the City of Calgary. The City monitors watershed runoff and snow conditions because the Elbow is a major source of drinking water and potable water can be a scarce resource during low flows.

The Elbow River watershed is 1210km² and is characterized by rolling to mountainous terrain. The eastern side of the watershed, around the community of Bragg Creek is generally flat terrain (maximum slopes of five degrees). The terrain increases in steepness towards the mountains in the west. The dominant vegetation types are trembling aspen, pine, white spruce, and heaths (Borneuf, 1980). The bedrock in the study site is dominated by the Tertiary Porcupine Hills Formation which consists of north-west to south-east units of non-marine sandstone imbedded with shale (Borneuf, 1980). The Elbow River lies in an old braided channel with recent deposits of sandy to coarse loam mixed with ribbons and bars of glaciofluvial gravel. Three glacial advances affected the Elbow River watershed. They are known as the Porcupine Hills the Maycroft Maunsell and the Erratics Train Glaciation (BSc Environmental Science, 2002). The latter of the three glaciation periods deposited most of the till in the Bragg Creek Valley. Since deglaciation, fluvial reworking and mass wasting have been the primary geomorphological forces affecting the region (BSc Environmental Science, 2002). The Elbow River watershed experiences 2314 hours of mean annual sunshine and averages 383mm of rain fall and 266mm of snowfall annually (Mitchell and Prepas, 1990; Environment Canada). Average precipitation for the province of Alberta

reports 389 mm of average rainfall, with 121mm of snow (Agriculture and Agri-Food Canada, 2000).

Location Map of Marmot and Elbow River Study Areas

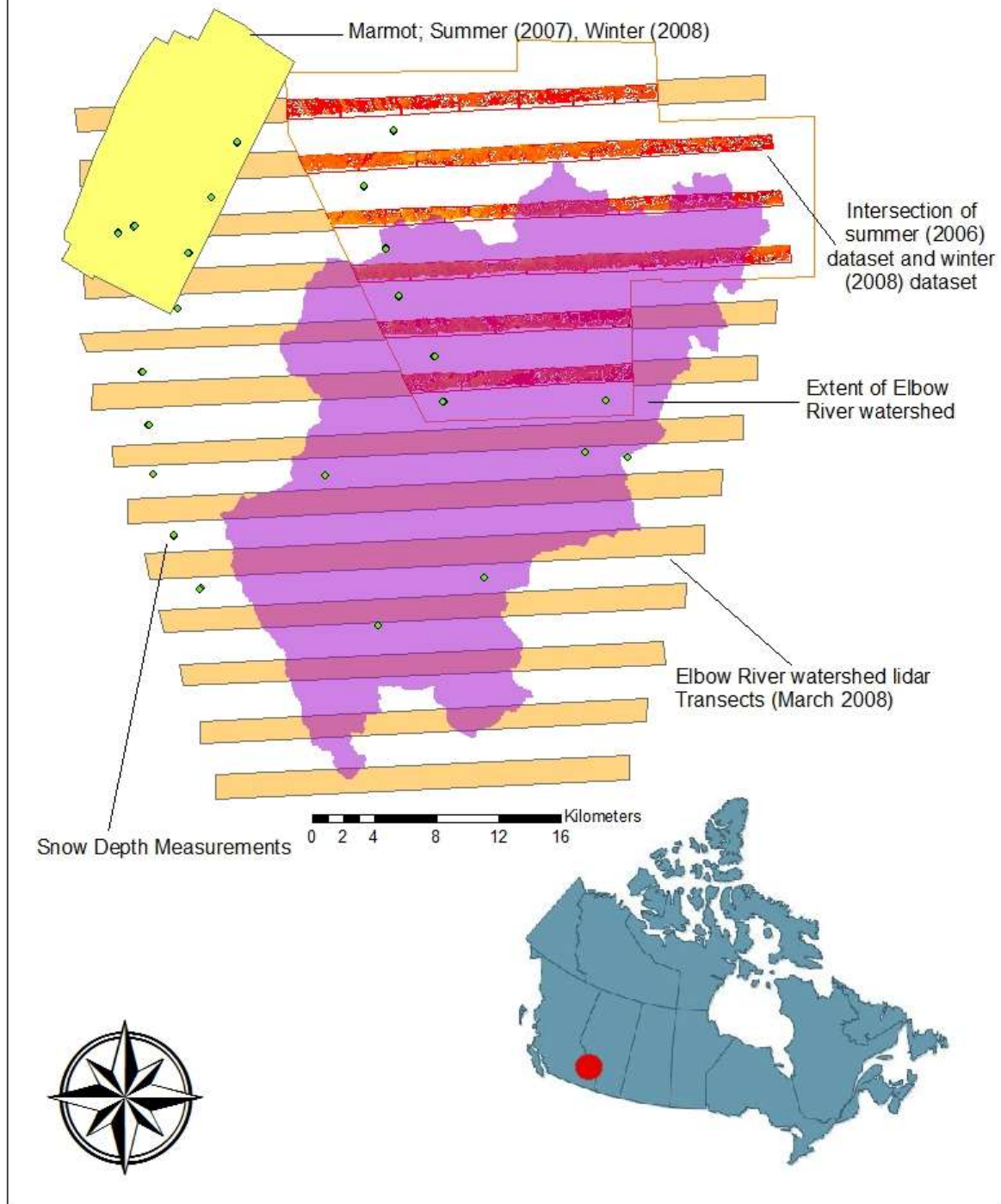


Figure 1: Study area location and airborne LiDAR survey transects over Elbow (orange swaths) and Marmot survey polygon (yellow polygon). Field sampling locations are illustrated as green markers.

Methods

Data Collection

Snowpack data collection took place in mid March, 2008 and was conducted by a team comprising members and resources from the Applied Geomatics research group (AGRG), Airborne Imaging, Sustainable Resources Development (SRD), Alberta Environmental Protection (AEP), University of Saskatchewan (U of S), and Wolf Survey. The March 2008 airborne LiDAR data collection over Marmot and Elbow was conducted by Airborne Imaging Inc. out of Calgary from March 22 to 24. From March 22 to 28, field personnel from AGRG, U of S, SRD and AEP were on the ground collecting snow depth transect validation data within both study sites. The field crew collected snow depth, slope, aspect, snow density and canopy fractional cover data at various survey grade GPS located transects within the study area. Conditions at the time of the winter data collections were generally clear, although there was some light snowfall in the middle of the campaign.

The non snow covered DEMs for the two sites were collected prior to the field campaign in two different missions and by two different agencies. The LiDAR data over Elbow and surrounding environment were provided by SRD but were originally collected by Airborne Imaging Inc in the summer of 2006. The 'no snow' LiDAR data over Marmot were collected by AGRG in August of 2007. All three LiDAR data collection campaigns utilized the same type of LiDAR sensor; an Optech Airborne Laser Terrain Mapper (ALTM) model 3100. The marmot study focused on establishing LiDAR-based terrain and canopy cover relationships with snow depth, while the focus at Elbow was in using LiDAR snow depth estimates and a GIS model to estimate watershed snow volume.

Figure 2 below illustrates the planned data collection strategy. While most of the field locations were visited and sampled by the AGRG team, the planned flight lines were flown with an offset of approx 2km by the Airborne Imaging team, leading to a lack of coincidence between field and LiDAR data over Elbow. The field snow depth data collected over the high elevation slopes of Marmot have not yet been made available to this study.

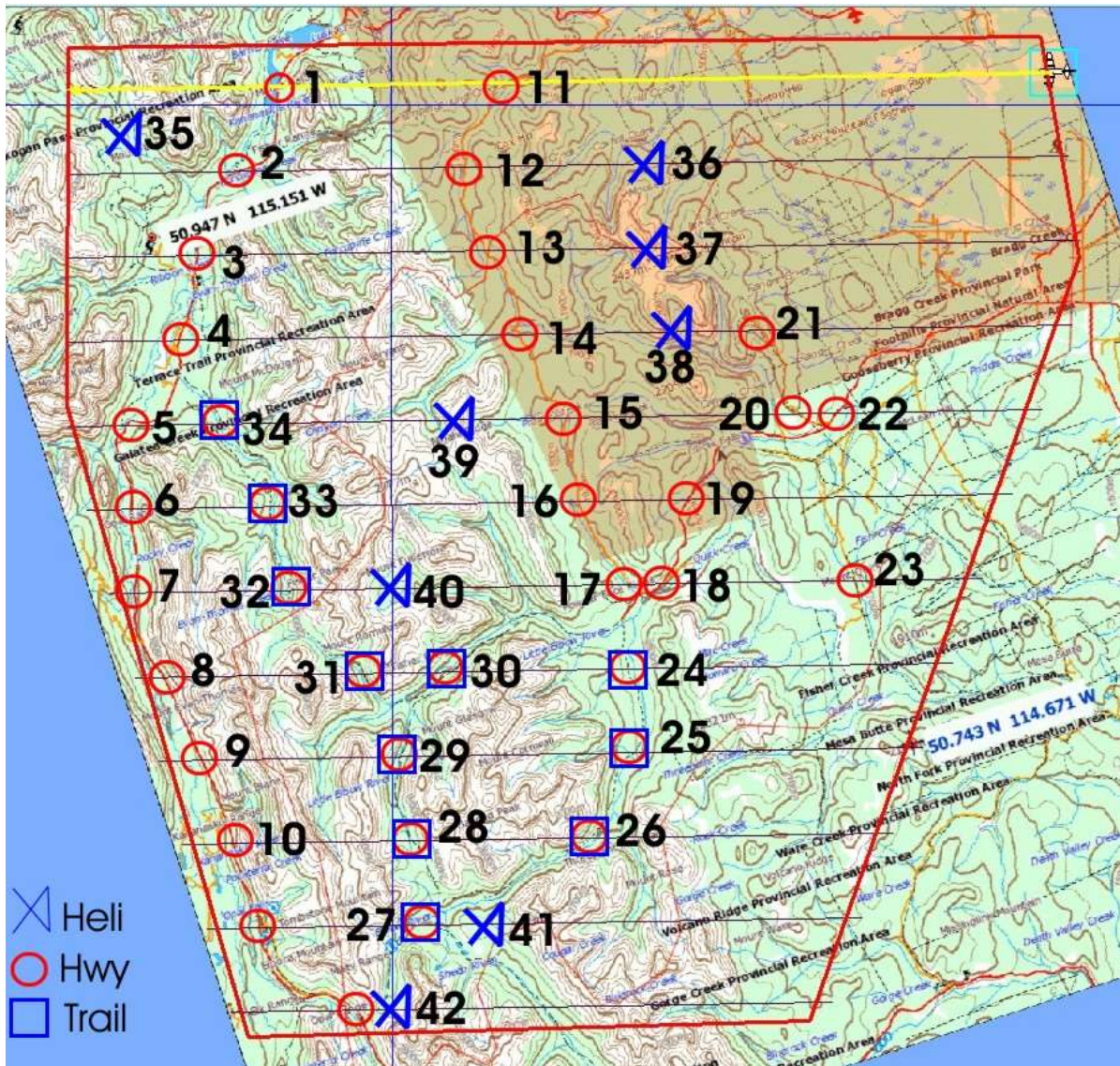


Figure 2. Proposed field and airborne data collection plan.

Figure 3 illustrates the data collection strategy adopted for snow depth and SWE estimation at each of the sampling locations. For each transect snow depth, snow water equivalent (SWE), aspect, slope and elevation data were collected. Digital Hemispherical Photographs (DHPs) were taken to estimate canopy fractional cover. DHPs are taken using a camera equipped with a 180 degree full hemisphere fisheye lens. The photos are used to measure the ratio of open sky to canopy foliage, otherwise known as canopy fractional cover (FC). The field data were stratified according to slope, aspect, elevation and fractional cover. These averages were compared to the averages computed from the LiDAR dataset to determine whether any correlation existed.

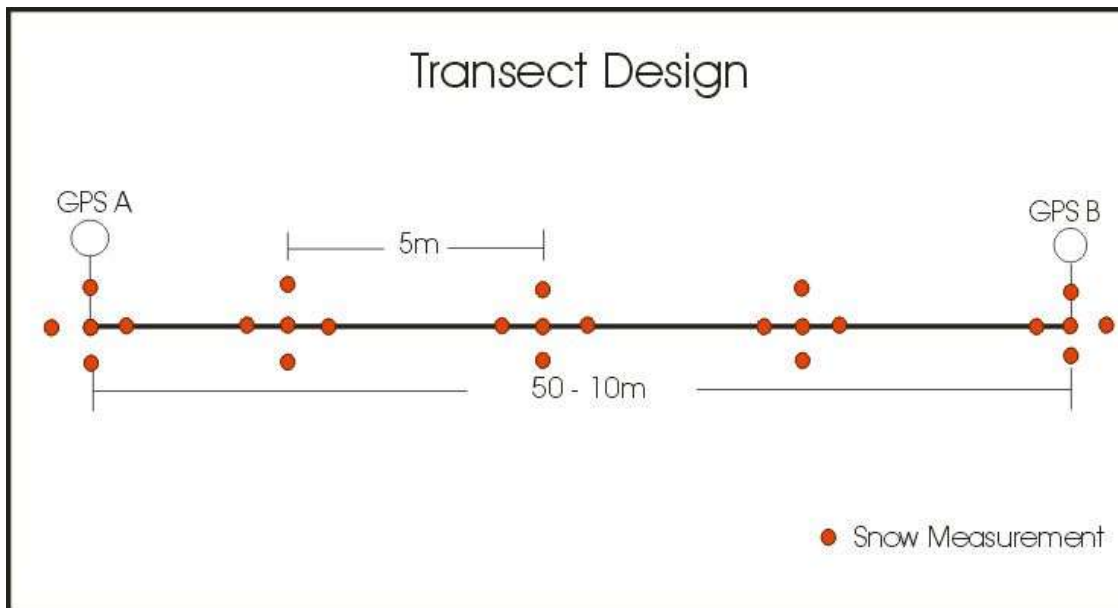
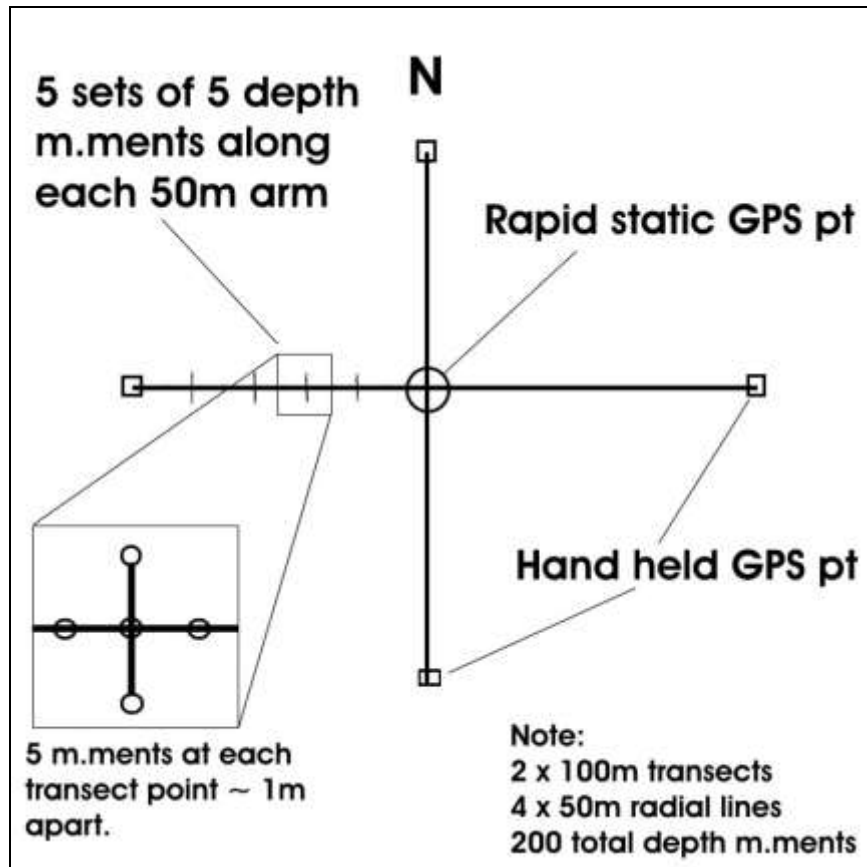


Figure 3. Field snow depth sampling designs. All transect GPS positions were differentially corrected to the base used for the airborne data collections. Four radial depth measurements were made 1m out from at each surveyed sampling location. Most transects followed the design outlined in the bottom diagram.

Multiple snow depth measurements were collected at each transect. The transect style chosen was a linear approach with snow depth measurements collected along its length (Figure 3). The linear transect allowed more study sites to be performed during the three days of field work. A typical transect was between 50 – 100m (using a 100m measuring tape) in length and usually included a transition zone from open to forested terrain. Snow measurements were performed at 5m intervals with a standard 1m aluminum measuring ruler (for snow depths over one metre, a survey range pole was utilized). At each interval five snow depth recordings were collected (centre, 1m north, south, east, and west) (Figure 3). The five snow depth recordings were averaged to obtain an average snow depth for each 5m interval.

Terrain attributes of aspect and slope for each transect were noted. The aspect of a slope was determined to be North, East, South, or West facing using a compass. Slope was determined on a scale of flat (0 – 22.5 degrees) and moderate (22.5 – 45 degrees). During the collection of the field data no data collection was performed on steep slopes (> 45 degrees). Upon returning to the lab, the snow depth measurements were stratified into the four cardinal directions for aspect, and flat and moderate for slope. The snow depths from each class were averaged to give an average snow depth.

Canopy cover was characterised in two ways. The first was to record where the canopy changed from open to closed canopy along the length of each transect. Therefore, for every snow depth measurement collected, an “open” or forested” attribute was assigned. The second method to determine canopy fractional cover was with the collection of Digital Hemispherical Photos (DHPs). DHPs were collected at the end points or midpoint of a transect. To collect DHPs the use of a digital camera equipped with a fish-eye lens was employed. The camera was set up on a tripod and raised to the height of 1.0m with the rear of the camera oriented north and the lens pointing vertically into the canopy. The 1.0m height requirement was chosen to eliminate as much of the understory brush from the image as possible. The purpose for orienting the camera north is that some DHP processing software requires a known north direction. Ideally DHPs are collected under a uniform sky, preferably just before sunrise or sunset or when the sky is evenly overcast (Bréda, 2003; Lovell *et al.*, 2003). However, due to the nature of time constraints associated with the field collection this was not possible to control.

Upon returning to the lab, snow depth was stratified into “open” vs. “forested” such that an average snow depth was acquired for both open and forested. Secondly, the DHPs were processed using the DHP processing software Caneye. A manual classification scheme was used to class the image into two classes: open sky and tree canopy. Caneye provided information on leaf area index (LAI), Gap fraction, and Fractional cover. The fractional cover for each photo was recorded and compared to the average snow depth at the location where the photo was acquired.

Snow Density was determined at most of the transect sites. The purpose of measuring snow density was so that snow water equivalent (SWE) could be estimated. SWE was calculated using the following expression (National Snow and Ice Data Centre):

$$\text{SWE} = \text{depth (m)} \times \text{density (kg/m}^3\text{)}$$

SWE in the field was measured using a weighing snow sampler. The graduated cylinder is pushed vertically through the snow to remove a snow core. The depth on the cylinder is recorded in meters. The core is weighed and the empty weight of the cylinder is subtracted from the total weight to acquire the snow weight. The area of the snow present in the cylinder is calculated by multiplying the snow depth in meters by the diameter of the cylinder (as stated by the manufacturer). The resulting snow volume is divided by the weight of the snow (kg) to achieve the snow's density. SWE is then easily calculated by multiplying the snow depth by the density.

To collocate the field and airborne data, differential survey grade GPS positions were acquired along each transect. The use of two Leica 530's and one Leica 1200 were employed during the course of the field collection. One GPS receiver was set up as a base station over a known benchmark at the University of Calgary's Research station in the Kananaskis Valley (less than 50km from study area and also used for aerial survey control) while the other two GPS units were operating as rovers in the field and later corrected to the base station. For transects measuring over 50m the roving GPS units were placed on either end of the transect, in shorter transects the GPS was set up in the middle of the transect. The GPS units were set up to collect static positions, and were left to acquire for 10 – 20 minutes depending on the canopy coverage (greater acquisition time for denser canopy).

The initial plan was to directly correlate snow depth measured on the ground with snow depth estimated from the LiDAR DEM subtraction method. However, the flight line data were not collected as planned and were offset by 2km, leading a lack of spatial registration between the field and airborne datasets. Even though the coordinates of transects are not used for spatial registration, the elevation from each transect was used to stratify the field collected snow depths by elevation.

LiDAR Processing and Snow Surface DEM Generation

The LiDAR data were combined with GPS and INS data to generate xyz data files of first, intermediate and last pulse returns. In theory, this allows the simultaneous collection of both canopy and ground surface points. In addition, the data were classified as either ground or vegetation returns using Terrascan software (Terrasolid, Finland), which uses an iterative windowed spatial filtering technique to classify the points. This classification procedure was applied to both survey data sets to remove the influence of vegetation so that the 'no snow' ground surface could be compared directly with the snowpack surface. Each data set was gridded to a 2 m raster matrix (using an Triangulated Irregular Network (TIN) interpolator) to facilitate DEM inter-comparison and volumetric calculations. A 2 m resolution was chosen to be commensurate with the raw data density. Following generation of the two DEM surfaces, snow pack depth maps were generated by subtracting the ground DEM from the snow surface DEM.

Analysis of Field and LiDAR Data

Data preparation involved cleaning, tiling, classifying, rasterizing and subtracting the `no snow` and `snow covered` DEMs in order to generate a map of snow pack depth. Three software packages were employed in the preparation of the LiDAR data: TerraScan, Golden Software Surfer, and ESRI Arcmap.

Terrascan

A) Upon receiving the two datasets (summer and winter) the first step was to identify the area of interest (AOI). In order to do a LiDAR snow pack analysis, an overlap between the summer and winter datasets must exist (refer to figure 1, the red rectangles represent the winter dataset, the orange block represents the summer dataset).

B) Once the overlap between the two datasets was determined a project file in TerraScan was created (dgn). Raw las files received from the LiDAR acquisition company are usually too large to work with efficiently; therefore a user defined tile system was created within TerraScan. For Elbow it was determined that the rectangular tiles that followed the LiDAR flight path would be optimal, while for Marmot 2km² tiles were adopted. Tile file size should be kept at a minimum (it has been found that Surfer using the TIN gridding algorithm will only handle file sizes of less than 100Mb). Once the tiles were created the summer LiDAR points were imported into the tiles. The winter datasets were imported using the same tiling scheme to ensure ease of comparison later.

C) Before comparing the winter and summer datasets it is very important to check for horizontal and vertical shifts. Due to the differences in the acquisition timing and specification of the two LiDAR datasets, shifts in x,y, z could be present resulting in the need for one of the datasets to be block adjusted. Observed offsets that are smaller than approximately 30cm are well within the combined noise level of the two datasets. Systematic shifts of more than 50cm require closer scrutiny and need to be corrected.

Shifts between the summer and winter datasets were calculated by loading two identical tiles into the same viewing window: the summer dataset was loaded into class 1 and the winter dataset into class 2. The result (as shown in Figure 4) represents the summer dataset point cloud in green and the winter dataset in red. The measuring tool within TerraScan was utilized to measure any apparent shifts between the two datasets.



Figure 4: Example of horizontal shift over building roof between summer and winter datasets

Horizontal shifts were determined with ease when buildings were available (due to the sharp edges of the buildings). However, the shift was not easily identifiable in the absence of obvious landmarks. Vertical shifts were determined by using flat roads as reference. For the Elbow transects, shifts were evaluated on a flight line by flight basis, while for marmot, the entire set was considered as a whole. After analysis of the Elbow dataset it was determined that two out of the six flight lines had enough buildings to determine a horizontal shift. Statistics calculated for this shift are shown in the appendices. A “bulk-shift” was applied to flight lines 4 and 5 on the winter dataset. The shift was applied to the winter dataset and not the summer for the reason that the summer dataset is a published government dataset and the winter LiDAR dataset was collected specifically for this particular study. The shift applied to the Marmot dataset was small and close to the noise level (50cm). The small value of the adjustment necessary for the Marmot dataset is thought due to using the same base station for both surveys in 2007 and 2008. However, the comparisons were only made in the valley locations in and around the highway and Kananaskis Village, as further to the west and at higher elevations, there were no objective and obviously equivalent surfaces that could be compared. Therefore, there remains the possibility of some slight mis-registration of the datasets at these higher elevations.

D) The next data preparation step was to perform a classification on both the summer and winter datasets. A classification of the two datasets separates the LiDAR return data in ground vs. non-ground points. By creating a ground class, all the points that are not associated with the ground (such as trees and buildings) are separated out of the dataset, since they are not required for the snow pack analysis. The “all hits” files are kept however, for later use in the calculation of canopy fractional cover.

E) After the ground classification and shifts have been applied to the datasets, the tiles were exported from las files to xyz files for further data preparation in Golden Surfer.

Golden Software Surfer

A) A 3D surface (Grid) of the ground classified tiles (summer and winter) was created using the gridding method Triangular Irregular Network (TIN). TIN was decided to be the best algorithm for this kind of dataset because the original LiDAR points were used to define the triangles, thus honoring the original Z values closely (Surfer Gridding, Golden Software). In addition, the TIN algorithm is relatively fast, and the datasets were large, so this was considered the most efficient approach to take. The gridding process was performed at a 1m cell size for Elbow and 2m for Marmot. The grid extents had to be exactly the same between the summer and winter datasets in order to perform math functions on the resulting grids.

B) Using the grid math function within Surfer a snow depth grid was created. Snow depth was calculated by subtracting the summer grid from the winter grid.

$$\text{Snow Depth} = \text{Summer Grid} - \text{Winter Grid}$$

C) Canopy fractional cover is one of the four terrain attributes that was examined for its effects on snow accumulation. Fractional cover estimates using LiDAR data were calculated using the following equation (Hopkinson and Chasmer, 2008):

$$\text{Canopy Fractional Cover} = \frac{\sum R_{\text{Canopy}}(\text{all})}{\sum R_{\text{Allhits}}(\text{all})}$$

Canopy fractional cover was computed by first performing a residual analysis on the winter ground grid using the “all hits” points from the winter dataset. The winter dataset was used to determine canopy fractional cover because snow accumulation occurred during leaf off conditions. The residual analysis created a column called “residuals” in the “all-hits” point file. This column represented the difference between the grid ground elevation and the elevation of a point at the same xy coordinate (the difference equates to canopy height). As the above equation shows canopy fraction cover is the division of the sum of the returns of the canopy by the sum of the returns of all returns. The “all-hits” grid was created by gridding the “all-hits” point file using the residual column as the elevation parameter. The gridding algorithm employed was Data Metrics using a 5x5m search radius and a 1m cell size for Elbow and 2m for Marmot. Likewise the canopy grid was created using the same procedure except it excludes all values under 1.5m. By excluding all returns under 1.5m, the data represents the tree canopy while excluding the canopy understory. Once the canopy and all hits grids were created, the above quotient was established using Surfers grid math function.

D) Once the summer, snow depth, and canopy fractional cover grids were created they had to be converted into ASCII (asc) files. ASCII files were created because Arcmap does not read Surfer grid files. The Surfer Scripter script grd2asc.bat was used to convert the Surfer grid

files into ASCII files. Surfer Scriptor scripts can be found at the following website:
<http://www.goldensoftware.com/scripts-S.shtml>.

Arcmap

A) The snow depth rasters were imported in Arcmap as raster grids.

B) Upon analyzing the snow depth and canopy fractional cover grids for the Elbow LiDAR transect data it was noticed that at the edge of the scan there were TIN interpolation errors. These errors were manifested as high or low depths and they had to be clipped out from the dataset. The clip was performed by digitising a polygon around the individual flight lines excluding the sensor error. By using the “Extract by Mask” tool within spatial analyst a new raster was created excluding the erroneous strip edges. (This step was unique to this particular dataset.)

C) All the tiles were mosaiced to create a single raster for data analysis. This process was performed for each dataset (summer, snow depth, and canopy fractional cover).

D) Canopy fractional cover over the Elbow area was re-classed into 5 classes (0-5%, 6-30%, 31-50%, 51-70%, and 71-100%). This class break down was chosen due to the available canopy data provided in the SRD GIS data layers for the Elbow River watershed, which uses the same 5 class categories. A different stratification was employed for Marmot: i) zero cover; ii) less than 30%; iii) 30% to 60%; iv) greater than 60%. This stratification was based on the need for an approximately even distribution of four canopy cover classes.

E) The elevation attribute class was created by taking the summer LiDAR dataset and re-classing it into 100m elevation bins. The summer dataset was used because it represents the “true” elevation. See Figure 5.

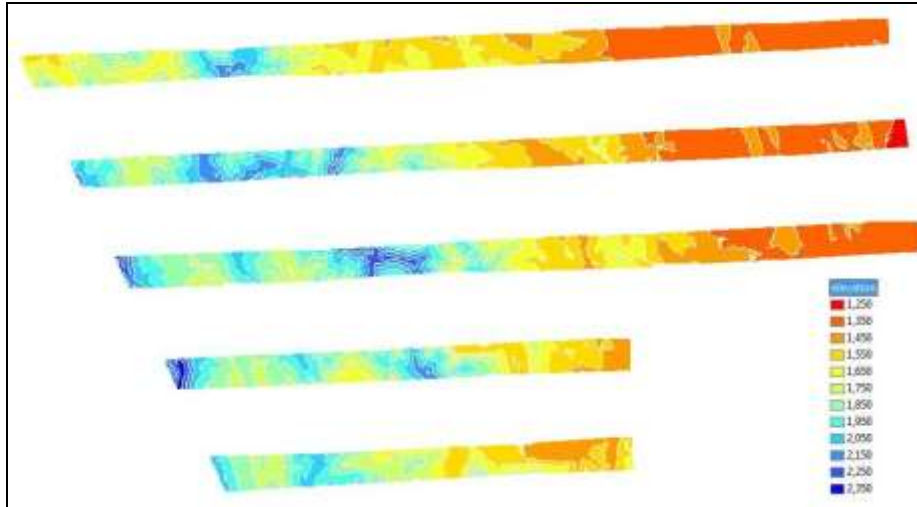


Figure 5: Example of Elbow Creek area LiDAR elevation dataset classed into 100m bins

F) Aspect was created using the aspect tool within spatial analyst. The input for this function is the summer LiDAR dataset. Aspect was stratified into the four cardinal directions (N,E,S,W). Aspect was tested, as it was hypothesized that north facing slopes would display deeper snowpack than south facing slopes as a result of differences in solar insolation.

G) Slope was created using the slope tool within spatial analyst. The input for this function was the summer LiDAR dataset. The output from the slope function was re-classed into the four categories for Elbow (0-22.5°, 22.5 - 45°, 45 – 67.5°, 67.5 - 90°) and three classes for marmot (0 to 30 degrees; 30 to 60 degrees; above 60 degrees). Slope was created with the summer dataset because the snow in the winter dataset masks the true values of the slope.

H) For Elbow, the snow depth raster was re-classed into 20cm bins from 0 – 4m, while for Marmot, depth was re-classed into 1cm bins to allow a higher resolution of analysis.

I) The final three categories of terrain stratification were Topographic Wetness Index (TWI), Terrain morphology (flat, upland, depression) and winter radiation load. These terrain attributes were only tested over Marmot, as they are slightly more sophisticated than those employed over Elbow and require additional DEM data processing. TWI and terrain morphology were tested, as it was believed that localized depressions in the landscape would incur deeper accumulations of snow. Winter radiation load, like aspect, was evaluated, as it was believed, deeper accumulations would occur in areas of minimal radiation input, and therefore melt and evaporation. TWI and terrain morphology were manually derived using the raster calculator functions in Arcmap. Total winter radiation load from December through to April was calculated using the solar analyst extension in Arcmap. TWI and radiation were stratified into even quantiles (33% each) of high, medium and low values, while morphology was stratified into flat, depression and upland classes. Snow depth for each of these terrain classifications were summarized using the zonal

statistics function in Arcmap. Examples of the terrain and landcover attributes that have been stratified for this analysis are presented in Figures 6 to 10 for the Marmot area below.

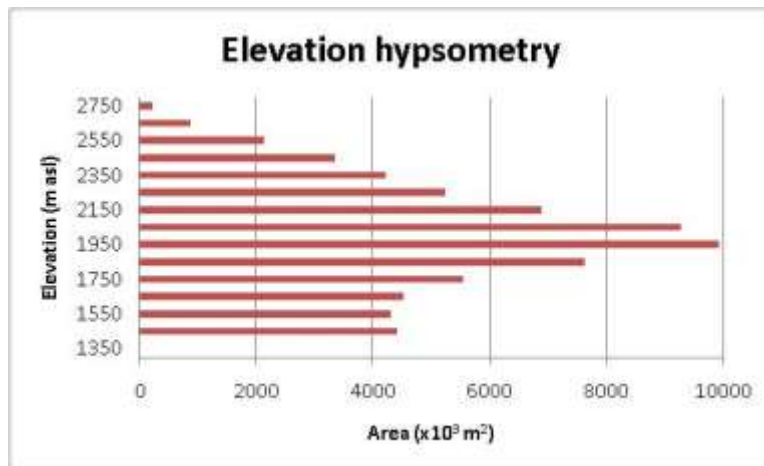


Figure 6. Elevation hypsometry of Marmot study area.

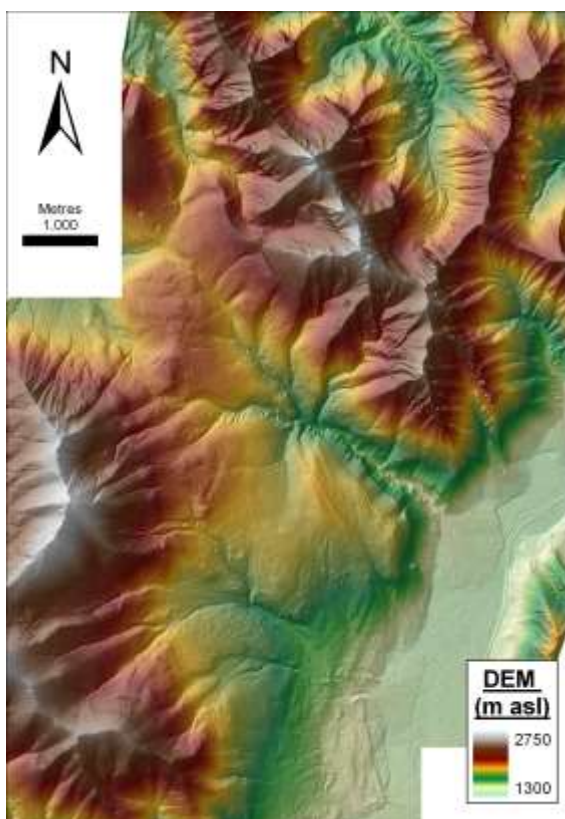


Figure 7. Marmot area digital elevation model

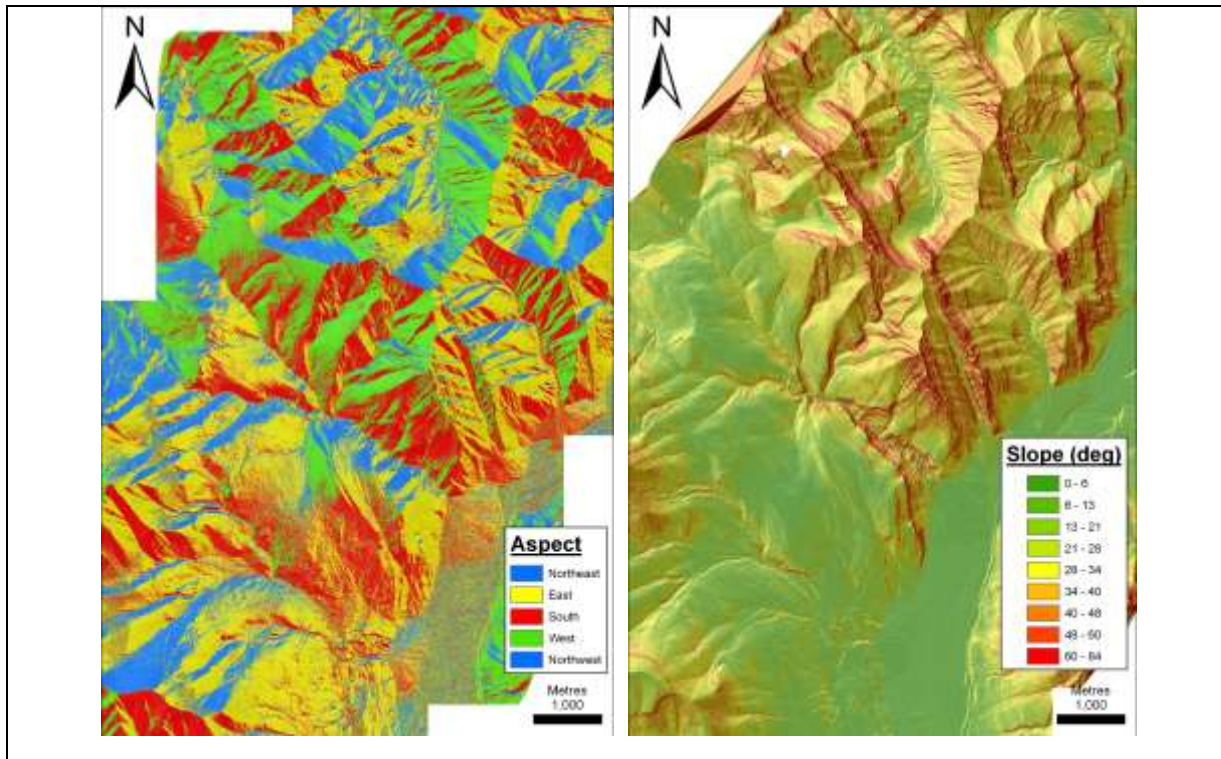


Figure 8. Marmot area aspect and slope maps.

It was believed that slope might play some role, as gravitational action distributes snow downwards from sloping terrain towards flat terrain but also because slopes can act as barriers or obstructions that must be negotiated during lateral distribution of snow that is being transported by wind.

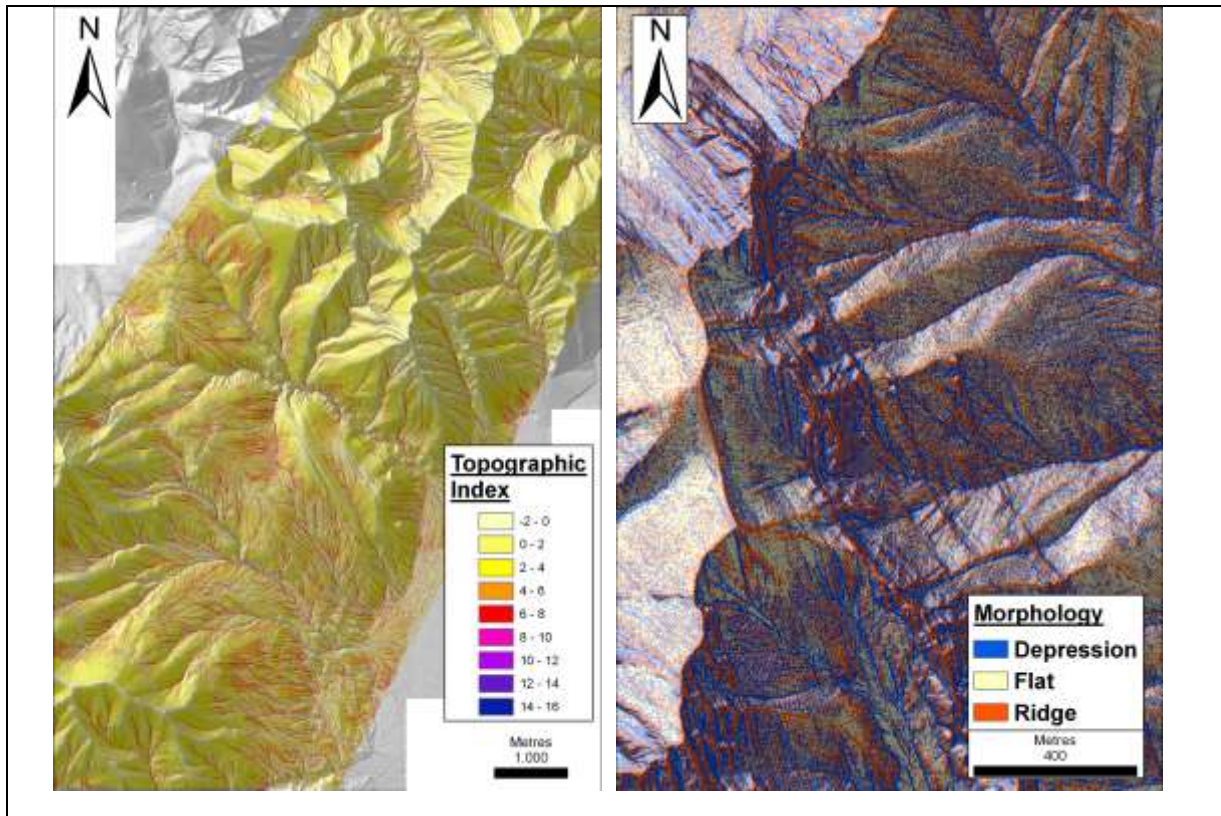


Figure 9. TWI and Terrain morphology.

Terrain morphology is stratified into localized uplands (ridges), flat areas, and depressions (gulleys). Both TWI and morphology were tested, as it was believed that snowpack would preferentially collect in depression areas due to the downward distribution of snow by gravity and wind action.

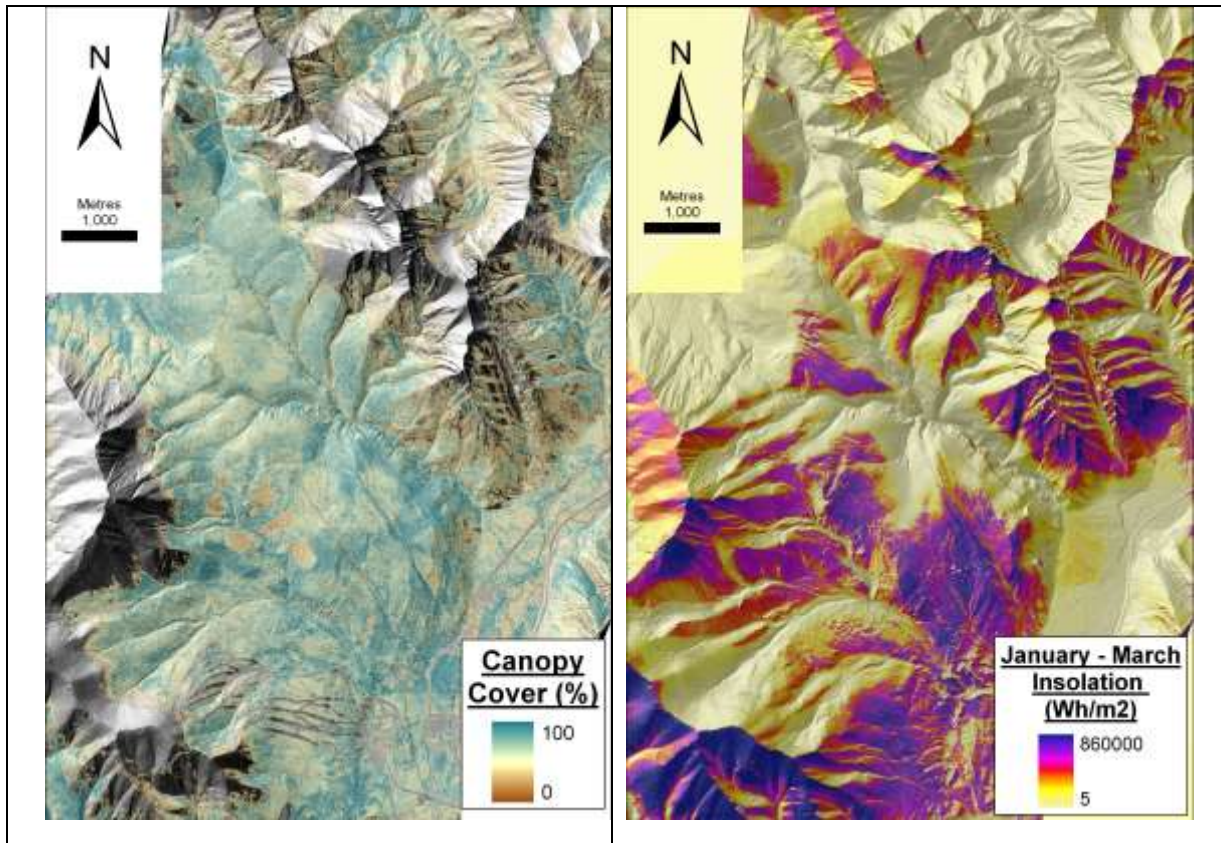


Figure 10. Canopy Fractional Cover (FC) and winter radiation load over Marmot Creek area.

Fractional canopy cover was tested, as it is generally observed that (all else being equal) snow depth accumulation is diminished in dense forest covered areas. Winter solar insolation was computed, as it is assumed that in areas of increased radiation, snow depth will reduce due to early melt out and or sublimation.

Creation of the Elbow Watershed

1) Access to a high resolution DEM was not available therefore a 90m DEM was utilized. 90m Shuttle Radar Topography Mission (SRTM) was available free of charge off the internet. The following are some sites where SRTM data can be acquired:

<http://srtm.csi.cgiar.org/SELECTION/inputCoord.asp>

<http://glcfapp.umiacs.umd.edu:8080/esdi/index.jsp>

<http://www.geobase.ca/geobase/en/>

2) The Elbow River watershed happened to lie between two DEM tiles; therefore the two tiles had to be mosaiced together. The SRTM DEM also had to be re-projected into NAD83 as well as re-sampled to 90m (the cell size was not exactly 90m).

3) Once the DEM was properly projected and of the correct cell size, the watershed extents had to be delineated. The watershed was computed using the hydrology tools within the spatial analyst package. In order to perform the analysis the coordinates of a stream gauge downstream of the Elbow River was required. Stream gauge data was found at the following website:

http://www.wsc.ec.gc.ca/StreamOrder/Reference_Index_e.cfm?StnNum=05BJ004

The stream gauge location used for this analysis was the Bragg Creek Gauge (670735.7m W, 5646861.0m N, z11 NAD83). The gauge location was not the most downstream gauge for the watershed; therefore the watershed delineated is not the full extent of the Elbow River watershed. The excluded area of the watershed is primarily flat (less than 5 degrees slope) with little observed snow accumulation, therefore not critical to this analysis. The clipped watershed extent is illustrated in Figure 11.

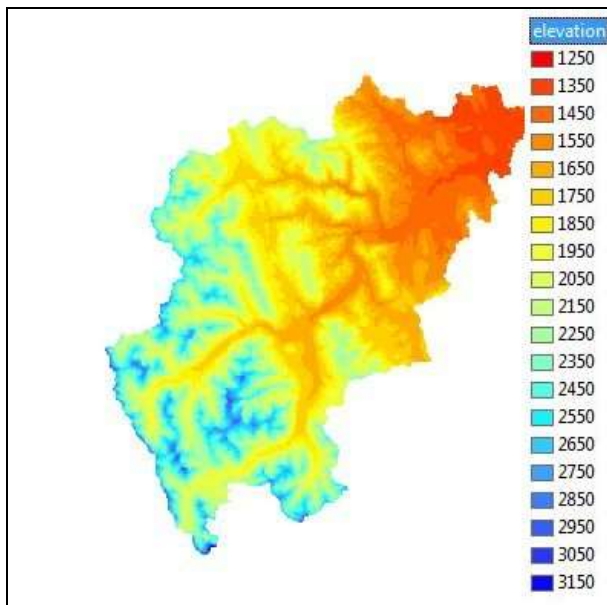


Figure 11: Elbow River watershed classified by elevation

4) The watershed analysis produces a polygon shape file of the extents of the Elbow River watershed. By using the extract by mask feature in spatial analyst the DEM was clipped to the extents of the watershed.

5) Using the same methods as described above, slope, aspect and elevation rasters were created.

6) Canopy fractional cover was available for the entire watershed from SRD's forest AVI attribute tables. The AVI attributes included crown closure for the entire coverage. Crown

closure from the AVI was validated by referencing it to DHP canopy fractional cover values collected in the field.

Snow water Equivalent field data results

The results of the SWE field data collection within the Elbow watershed are provided in the table below. Despite the wide range of canopy conditions and elevations, SWE did not vary significantly, with a mean value of 24% (SD=4%) (Table 1).

Snow Water Equivalent Elbow and Marmot			
Transect	Snow Depth (m)	Weight (mm)	%
11A	0.35	8.2	23
11B	0.6	16	27
12A	0.45	10	22
12B	0.57	12	21
13A	0.4	8	20
13B	0.27	8	30
14A	0.51	11	22
14B	0.55	12	22
15A	0.2	6	30
15B	0.39	8	21
16A	0.57	10	18
16B	0.37	11	30
		Average:	24%
		SD:	4%

Table 1. Snow Water Equivalent sampling results from Elbow Watershed.

Marmot Creek area field & LiDAR snowpack depth distribution observations

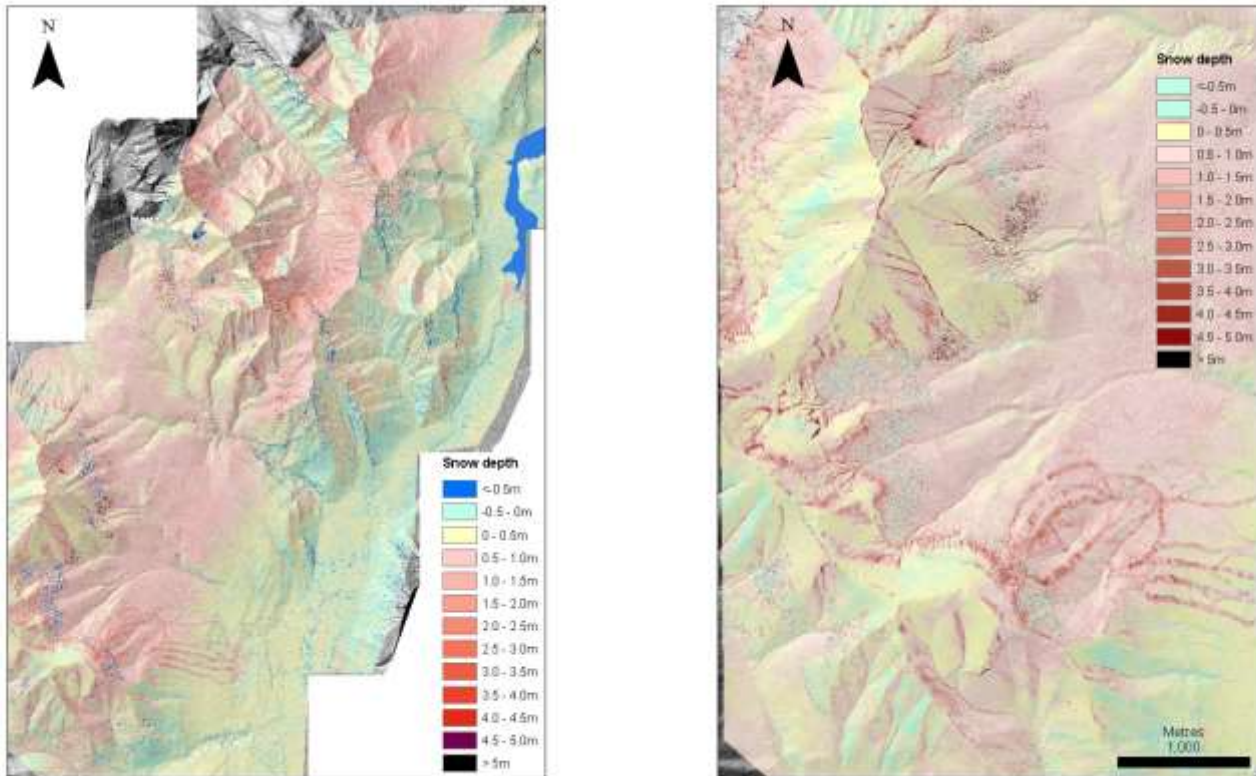


Figure 12. Spatial variation of snow depth over the Marmot creek and Nakiska ski hill area. Note deeper snow evident in tree lined ski runs at south end of image

The snow depth distribution maps over Marmot area (Figure 12) illustrate areas of increased snow depth over ski hill runs, within gulleys and at tree line. Reduced depths at highest elevations, presumably due to wind and gravitational distribution is also evident; clearly demonstrating that on average snow depth does not increase with elevation above tree line. It also appears that snow depth is enhanced on the western side of the slopes, presumably as a result of orographic effects and precipitation shadow. However, potential uncertainties due to LiDAR flight line errors cannot be discounted, as the flight lines were oriented parallel to the axis of the mountain chain.

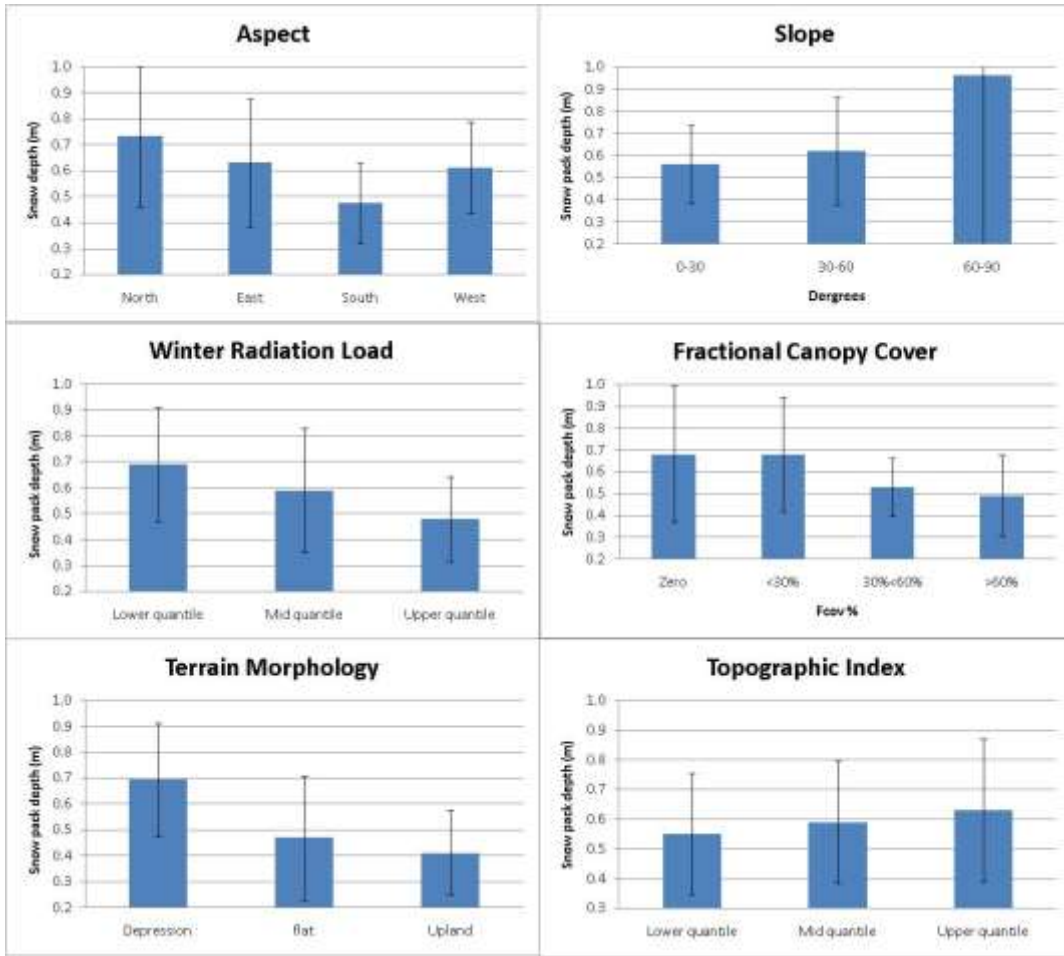


Figure 13. Marmot area snow depth stratification by terrain and landcover attribute. (Error bars represent the data variance).

Terrain attributes		Snow depth (m)		
		Mean	Difference	Std Dev
Morphology	Depression	0.69		0.55
	Upland	0.41	0.28	0.51
Aspect	North	0.73		0.52
	South	0.47	0.26	0.39
Radiation	Lower quantile	0.69		0.47
	Upper quantile	0.48	0.21	0.40
Fractional cover	<30%	0.68		0.54
	>30%	0.52	0.15	0.38
Topographic Index	Lower quantile	0.56		0.45
	Upper quantile	0.63	-0.08	0.49
Slope	< 30deg	0.56		0.42
	> 30deg	0.63	-0.07	0.51

Table 2. Summary statistics of snow depth by terrain and landcover attribute.

Comparative plots for all major land cover and terrain attributes tested are presented in Figure 13 and Table 2. The terrain attributes are ranked from top to bottom according to the magnitude of difference in the mean snowpack depth.

We find that the greatest control (other than elevation) is terrain morphology; i.e. deep snow in depressions vs. shallow snow in ridges or upland areas. Aspect and radiation demonstrate similar results and this is to be expected given they are essentially autocorrelated with each other. Then canopy cover, with open canopy demonstrating 15cm deeper snow on average than canopy covered areas. Interestingly topographic wetness index and slope display only minimal controls (all differences are significant at the 99% level of confidence).

Elevation (m asl)	Snow depth (m)	
	Mean	Std Dev
1300-1500	0.19	0.16
1500-1600	0.28	0.26
1600-1700	0.37	0.31
1700-1800	0.54	0.35
1800-1900	0.66	0.36
1900-2000	0.67	0.38
2000-2100	0.73	0.42
2100-2200	0.91	0.56
2200-2300	0.77	0.51
2300-2400	0.78	0.63
2400-2500	0.69	0.51
2500-2800	0.75	0.51

Table 3. Snow depth with elevation

Elevation (Table 3.) exerts the dominant control on snow depth up to tree line, with an apparent reduction in the elevation gradient once tree line is encountered. In the regression plot to the right, a quadratic model provides a good prediction of snow depth with elevation but in reality, it is believed that the relationships is linear up to tree line and then snow depth evens out.

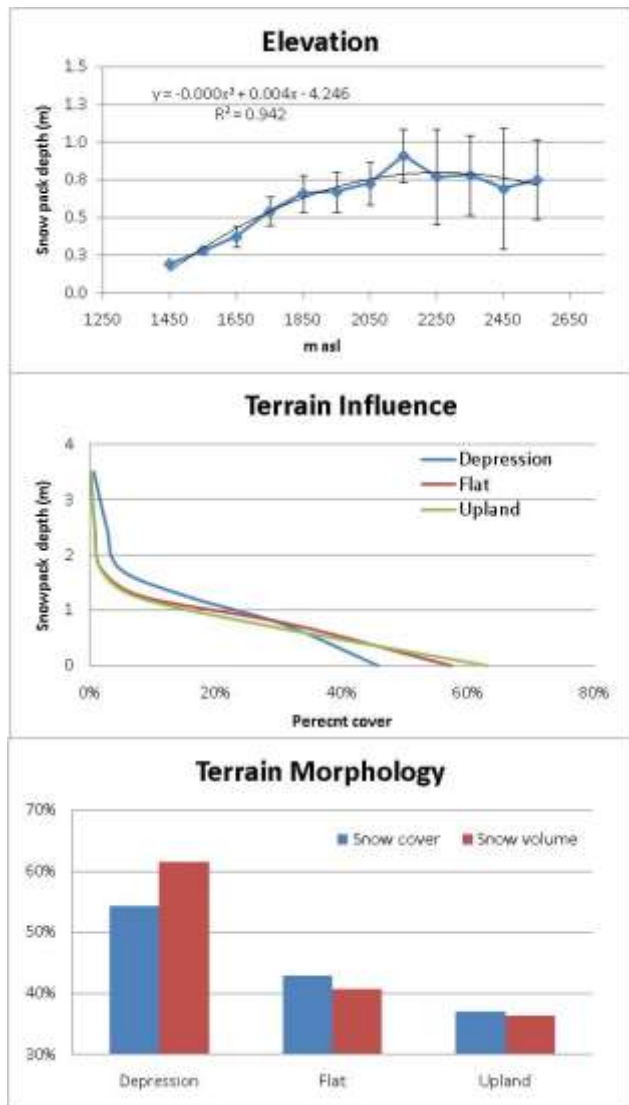


Figure 14. Snow depth with elevation and terrain.

The second dominant control on snow depth is morphology. This is evident in the plots above (Figure 14) where we see that both snow cover and snow volume reduce substantially (by almost 50%) from depressions to upland environments. We also see that less than 50% of depression areas display no snow cover at all, while for uplands, the proportion of zero snow depth approaches 70%. Finally, the deepest snow packs of 2m and above are only experienced in depression environments.

Elbow watershed field and lidar snowpack depth distribution observations

For Elbow, it was possible to compare both field and LiDAR estimates of snow depth stratified by terrain or canopy cover. However, due to the lack of coincidence of the airborne and field transect locations, we can only compare sample statistics rather than perform any direct correlations. The average of all snow depth from all 22 field transect was 0.28m (SD ~0.27m, n = 1675). However, this estimate cannot be applied to total watershed estimates of snow volume, as much of the ground cover was bare and thus had a depth of 0cm. While zero values were recorded in the transects and thus used in the calculation of average transect snow depth, the transects themselves were only collected in areas where snow cover existed. Thus, while efforts were made to represent varying landcovers and terrains, the transects are systematically biased towards representing areas where snow cover exists. Therefore, the field based estimate of snow depth provides a systematic overestimate at the landscape scale, and in order to correct this the average depth needs to be combined with a watershed estimate of snow covered area (SCA). Such data were not available for this study, as it would be impossible to accurately characterise snow cover proportion for such large areas of differing land cover and terrain type without some supplemental data.

The lidar estimates of snow depth were calculated by registering and then comparing the surface DEMs from 2006 (no snow) and 2008 (snow). The 2006 lidar data were provided by SRD and the 2008 data were collected by Airborne Imaging in partnership with AGRG on March 22nd of 2008 near the end of winter when snowpack conditions were marginal and not ideal for this experiment. The complete landcover estimate of average snow cover depth was 0.18m. This was smaller than the field transect estimate, as 100% of the landcover was used in the estimate; i.e. all area deemed to have no snow cover (i.e. 0.0m depth) were used in the calculation of LiDAR snow depth. If only snow covered areas are considered (due to the inherent noise in the data this is defined as any areas displaying more than 5cm positive depth), then the average LiDAR snow depth becomes 0.26m, which is very close to the field estimate.

Below are the summaries of snow depth distribution stratified by terrain and canopy cover attributes. Both the field and lidar based estimates are provided.

Elevation:

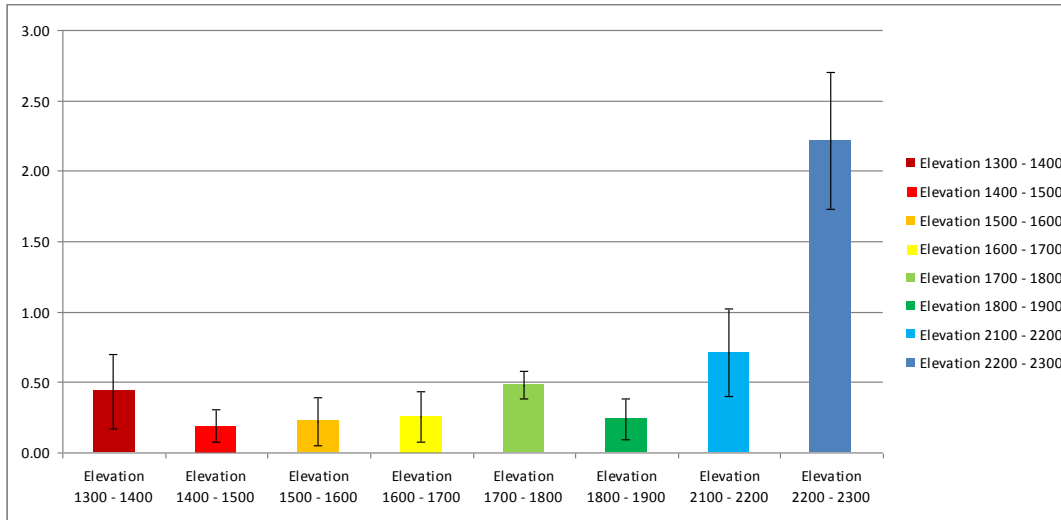


Figure 15. Mean field snow depth stratified by elevation (error bars = 1 standard deviation).

While there is some evidence of increasing snow depth with elevation in the field data (Figure 15), the two upper elevation samples are each represented by a single transect through relatively deep snow in localized depressions. Therefore, this plot cannot be assumed to provide conclusive evidence of a systematic elevation gradient in snow depth.

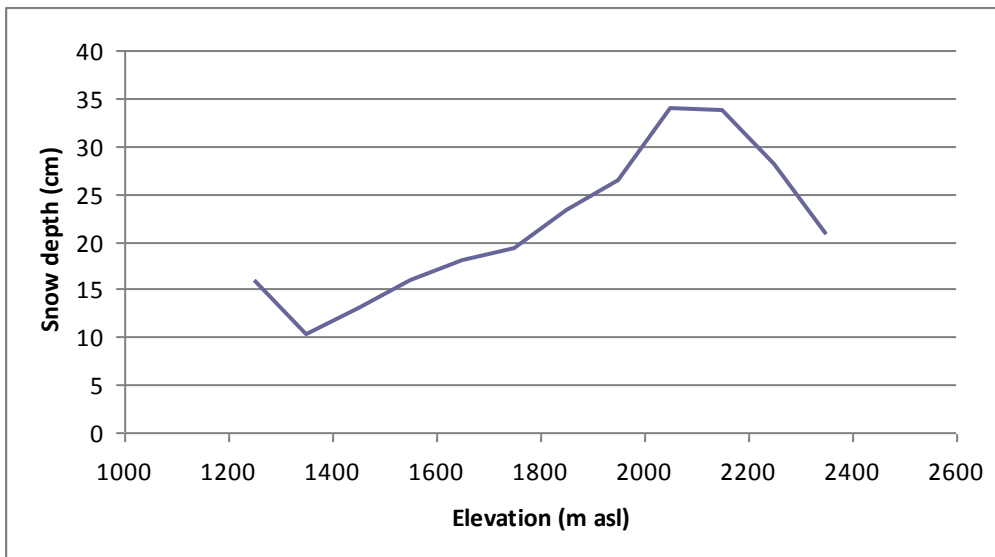


Figure 16. Mean LiDAR snow depth stratified by elevation.

As elevation increases LiDAR estimated snow depth increases across most of the elevation range (Figure 16). The graph shows a decrease in snow depth between 2200 and 2400m asl. This reduction in snow depth is believed due to downward distribution of snowpack over high exposed

mountain slopes above the tree line. As with the Marmot area data, maximum snowpack depth appears to occur around the regional treeline elevation between 2000 and 2200 m asl. The slight increase in depth at the lowest elevation range is believed to be due to outlying data in valley locations; the area of terrain represented within this elevation range is less than 1% and thus does not constitute a significant proportion of land cover.

Slope:

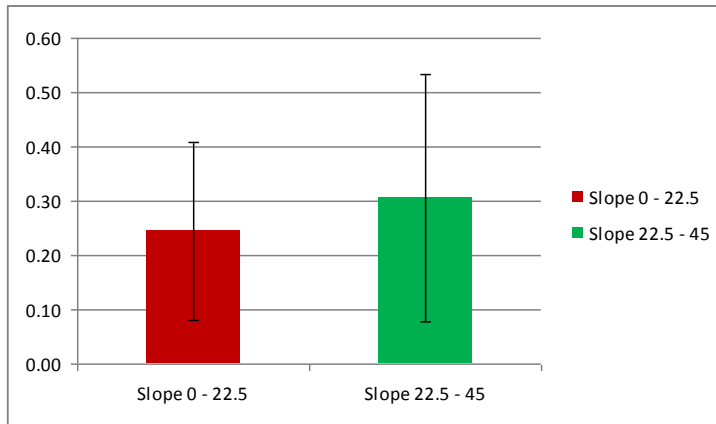


Figure 17. Mean field snow depth stratified by slope angle (error bars = 1 standard deviation).

The field transect stratification of snow depth does demonstrate a small but insignificant difference in depth with slope angle (Figure 17). No field data were collected from steeper slopes above 45 degrees.

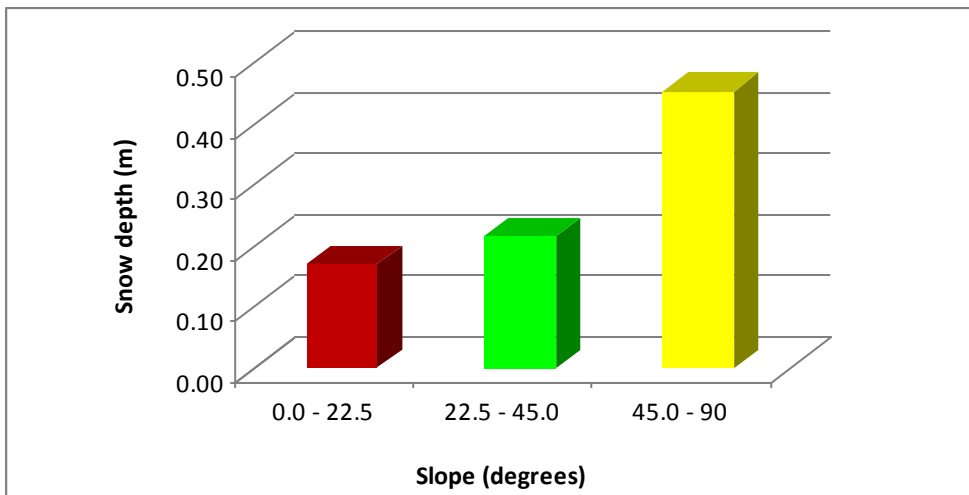


Figure 18. Mean LiDAR snow depth stratified by elevation.

A similar pattern is evident in the lidar data of increasing snowpack depth with slope angle (Figure 18). However, as with the Marmot data, we suspect some of this observed

increased depth at high slope angles is due to systematically increasing lidar DEM errors with slope.

Aspect:

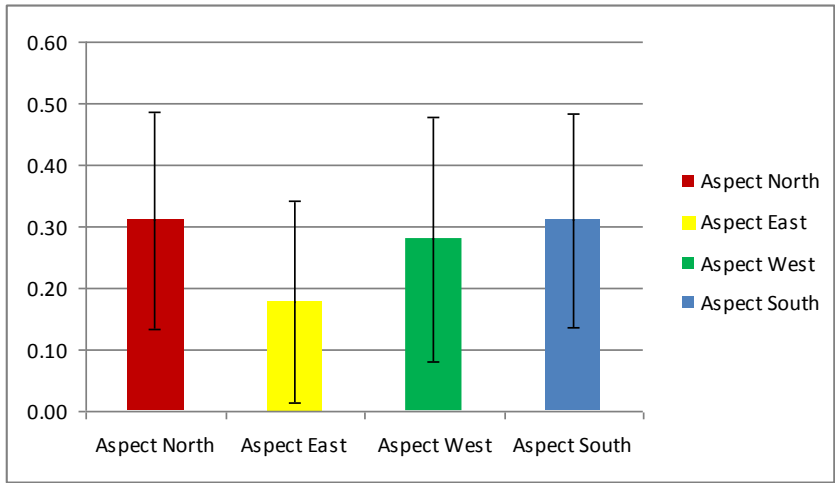


Figure 19. Mean field snow depth stratified by aspect (error bars = 1 standard deviation).

The field transect stratification of snow depth does suggest that north facing slopes possess the deepest snowpack depths but contrary to expectation, the south facing slopes illustrate depths that are almost as deep (Figure 19). This is thought to reflect the tendency for transect data to be collected in accessible valley locations that are typically shaded from winter solar illumination on all slopes. Also, much of the data was collected under canopy cover, where solar intensity would have been radically reduced. For these reasons, it is believed that the field data do not accurately capture the regional variation in snow depth due to aspect and radiation.

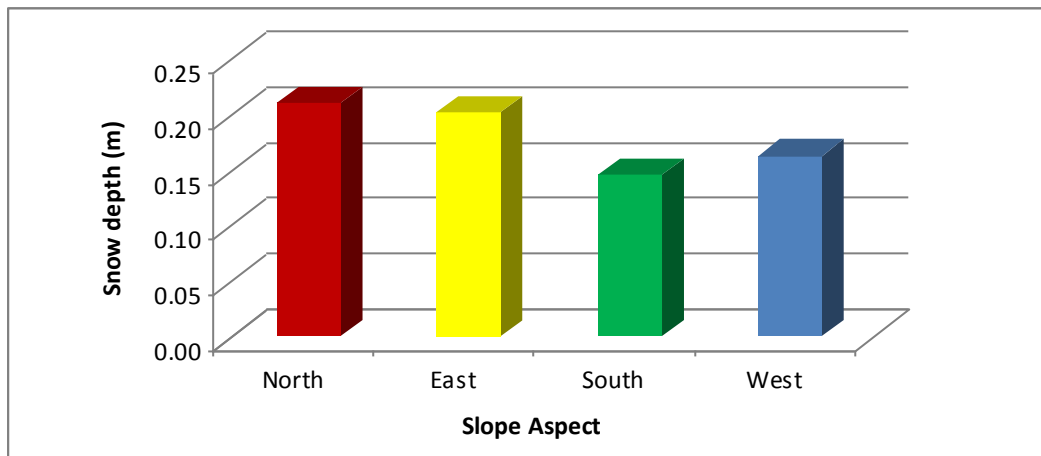


Figure 20. Mean LiDAR snow depth stratified by aspect.

Similar to the Marmot LiDAR snow depth data, we see a stratification in the Elbow lidar data such that depth is greatest on north facing slopes and shallowest on south facing slopes (Figure 20). This is as expected and provides further evidence that lidar is able to capture the distribution of snow depth patterns at the regional scale.

Canopy Cover:

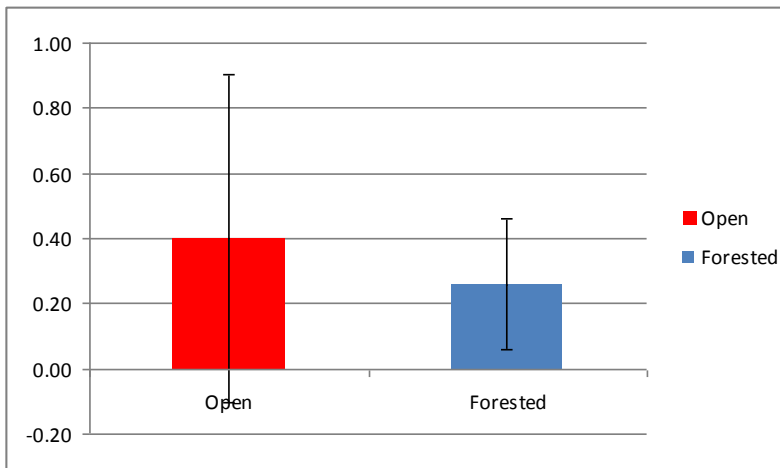


Figure 21. Mean field snow depth stratified by canopy cover (error bars = 1 standard deviation).

As expected, canopy cover was found to exert a noticeable impact on snowpack depth, with open areas generally demonstrating deeper snow depth (Figure 21).

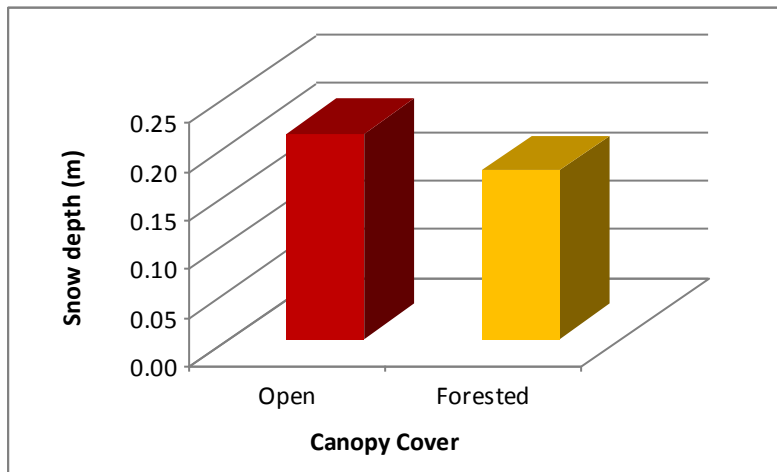


Figure 22. Mean field snow depth stratified by elevation (error bars = 1 standard deviation).

The same general pattern is evident in the lidar data at Elbow as with Marmot (Figure 22); i.e. when the fractional canopy cover is thresholded at 30% cover, we find that open canopies tend to have deeper snowpack than more dense canopy cover. The difference, in the Elbow dataset is only 4cm, however, and is not statistically significant.

Regional or west to east gradient effects:

An analysis was performed to determine if precipitation shadow effect was playing a noticeable role within the Elbow River watershed. Due to physical limitations in field sampling it was not possible to capture any regional trends in snowpack depth from field transect data. However, such a test was possible using the LiDAR data. The LiDAR snow depth transect data were separated into blocks of 3km in width running west to east over a distance of just over 30km. The goal was to determine if greater snow accumulation was apparent over the more mountainous part of the watershed in the west and less in the lower lying foot hill regions in the east.

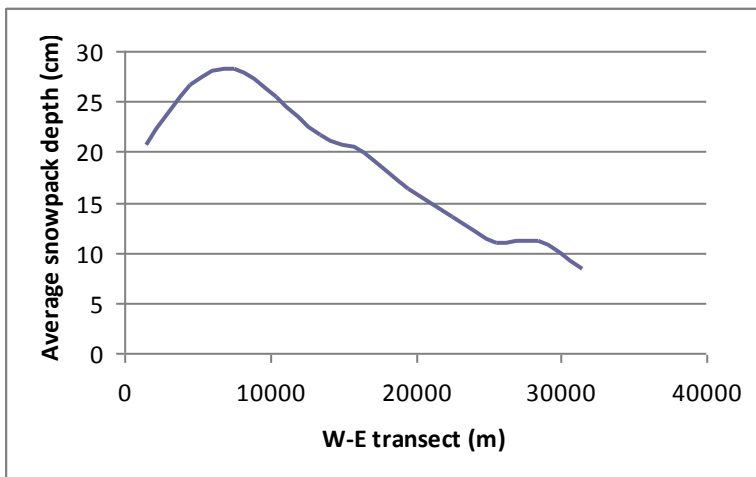


Figure 23. West to east gradient in LiDAR-based snow depth.

In Figure 23 we see the precipitation shadow effect combined with the elevation effect such that snowpack depth in the LiDAR transects is greatest at the high elevation western extremity of the watershed and smallest in the low elevation eastern slopes near the basin outlet at Bragg Creek.

Elbow Watershed LiDAR-based snow volume estimation

A number of snow volume calculation methods were attempted to provide some estimate of variability and therefore reliability in the overall efficacy for LiDAR- and GIS-based approaches to mountainous snowpack volume assessment.

The simplest approach was to apply the mean LiDAR snow depth to the entire area of the watershed (799km²). Then, each of the watershed attribute stratifications highlighted above were applied based segmenting the watershed into the associated landcover proportions. Finally, a hierarchical GIS model which segmented the basin into 12 classes based elevation (high, intermediate and low), aspect (north or south) and canopy cover (open or closed) was applied based on the observed depths for each strata within the LiDAR transect data.

Average snow depth method

A) A snow depth raster was created by the subtraction of the summer LiDAR dataset from the winter LiDAR dataset. Average snow depth was calculated by dividing the cell pixel count of each bin (20cm snow depth bins) by the total number of pixels, then multiplying that percentage by the snow depth of that bin. The resulting value represents an average snow depth for a given bin. All snow depth bins are summed together to get an average snow depth for the entire LiDAR dataset.

B) The average snow depth calculated from step A (18cm) is then multiplied across the entire watershed. The pixel size for the watershed dataset is 90m x 90m equaling 8100m². 8100m² is multiplied by the amount of pixels in the derived watershed (98644) for a resulting area of 799km². The total area of the watershed is then multiplied by the average snow depth derived from the LiDAR dataset to achieve an estimate of the total snow volume for the Elbow River watershed.

After applying the average LiDAR snow depth of 18cm to the entire area of the watershed the total snow pack volume was estimated to be 143,822,952 m³. Using the average snow density measurement collected at field transects the watershed SWE came to 33,079,279m³.

Average Snow Water Equivalent						
Average Snow Depth	Number of pixels in watershed	Pixel Size (90x90m)	Snow Volume (m ³)	SWE	Water Volume (m ³)	
0.18	98644	8100	143822952	0.24	34517508	

Table 4. Snow water equivalent estimation for the Elbow River watershed

Average snow depth by watershed attributes

The four watershed attributes investigated above were each individually chosen to predict total snowpack volume in the watershed. All four were used to give some idea of the range of volumes that might be expected.

A) In Arcmap, load the snow depth raster and one of the terrain attribute or canopy fractional cover (watershed attribute) rasters. Using snow depth as the first input and the watershed attribute as the second input perform the “tabulate area” function in spatial analyst. The resulting table gives a breakdown of pixel counts per category.

An average snow depth is calculated per class. First, all pixel counts are summed together for a total pixel count. Next each cell is divided by the total amount of pixels. This equals a percentage of the total number of cells. The percentage value is then multiplied by the snow depth to equal an average snow depth per cell. All the cells per terrain class are then summed together and divided by the area percentage for an average snow depth per class.

B) The next step was to make four estimates of water volume for the entire Elbow River watershed. By opening the attribute table for each raster a pixel count was provided for each terrain class. For example the aspect raster contains 24859, 31714, 20861, and 21202 pixels in the North, East, South, West classes respectively. By multiplying these pixel counts by the SRTM pixel size of 8100m² the area per direction is acquired. Multiplying the resulting class area by the class snow depth average will give an estimate of snow depth for that class. Summing all classes together generates an estimate for the entire watershed (see Table 5).

Note: The comparative LiDAR elevation datasets for Elbow in 2006 and 2008 do not cover any terrain that has an elevation exceeding 2400 m a.s.l. The Elbow River watershed is represented by elevations up to 3200m. For this simulation, and to ensure a range of snow volume estimates, snow depth was assumed to increase linearly with elevation. This, despite our assumption that this is not, in fact, the case.

Snow Water Equivalent Calculated By Individual Terrain Attributes							
Aspect	Pixel Count	% Area	Pixel Size (90m *90m)	Area (m ²)	Avg Snow Depth (m)	Volume (m ³)	SWE (24%)
North	24859	25%	8100	201357900	0.21	42774964	
East	31714	32%		256883400	0.20	52057965	
South	20861	21%		168974100	0.15	24770534	
West	21202	21%		171736200	0.16	28181647	
Total Area	98636				Total Volume	147785109	35468426
Slope	Pixel Count	% Area	Pixel Size (90m *90m)	Area (m ²)	Avg Snow Depth (m)	Volume (m ³)	SWE (24%)
0 - 22.5	68245	69%	8100	552784500	0.17	93309019	
22.5 - 45.0	28303	29%		229254300	0.22	49651342	
45.0 - 67.5	2086	2%		16896600	0.38	6345392	
67.5 - 90.0	10	0%		8100	1.31	106460	
Total Area	98644				Total Volume	149412213	35858931
Elevation	Pixel Count	% Area	Pixel Size (90m *90m)	Area (m ²)	Avg Snow Depth (m)	Volume (m ³)	SWE (24%)
1200 - 1300	2	0%	8100	16200	0.16	2576	
1300 - 1400	4302	4%		34846200	0.10	3594852	
1400 - 1500	7038	7%		57007800	0.13	7356986	
1500 - 1600	7990	8%		64719000	0.16	10246761	
1600 - 1700	8848	9%		71668800	0.18	12969237	
1700 - 1800	11312	11%		91627200	0.19	17573152	
1800 - 1900	9728	10%		78796800	0.23	18323708	
1900 - 2000	8522	9%		69028200	0.26	18255578	
2000 - 2100	8674	9%		70259400	0.34	23785334	
2100 - 2200	8568	9%		69400800	0.34	23357352	
2200 - 2300	7163	7%		58020300	0.28	16321995	
2300 - 2400	5931	6%		48041100	0.21	9994136	
2400 - 2500	4343	4%		22833900	0.42	9533153	
2500 - 2600	2819	3%		22833900	0.45	10218170	
2600 - 2700	1823	2%		14766300	0.48	7050908	
2700 - 2800	1030	1%		8343000	0.51	4234073	
2800 - 2900	435	0%		3523500	0.54	1893881	
2900 - 3000	91	0%		737100	0.57	418304	
3000 - 3100	16	0%		129600	0.60	77436	
3100 - 3200	9	0%		72900	0.63	45745	
Total Area	98644				Total Volume	195253338	46860801
Fractional Cover	Pixel Count	% Area	Pixel Size (90m *90m)	Area (m ²)	Avg Snow Depth (m)	Volume (m ³)	SWE (24%)
0 - 0.06	38647	40%	8100	313040700	0.20	62128570	
0.06 - 0.3	5666	6%		45894600	0.26	12051250	
0.3 - 0.5	13109	14%		106182900	0.19	20215825	
0.51 - 0.7	23839	25%		193095900	0.16	30928719	
0.71 - 1.0	14987	16%		121394700	0.17	20446095	
Total Area	96248				Total Volume	145770458	34984910
Canopy Cover	Pixel Count	% Area	Pixel Size (90m *90m)	Area (m ²)	Avg Snow Depth (m)	Volume (m ³)	SWE (24%)
Open	44313	46%	8100	358935300	0.21	75376413	
Forest	51935	54%		420673500	0.17	71514495	
Total Area	96248				Total Volume	146890908	35253818

Table 5. Snow water equivalent estimation for the Elbow River watershed (four terrain attributes)

GIS Model

The final water volume estimate explored in this project is a multiple terrain attribute GIS model. A hierarchical model using three of the four watershed attributes evaluated was created based on the understanding that snow pack accumulation is a result of multiple inter-related processes. Elevation, aspect, and canopy fractional cover were chosen as the three watershed attributes, as these demonstrated the most significant influences in prior analysis. The model is not physical or dynamic and makes no attempt to accurately represent snowpack distribution processes. The model predicted average snow depth based on establishing, and then applying, average snow depth for each of twelve possible combinations of the of the three terrain attributes. Elevation was classed into three classes (high, medium, low); aspect into two classes (North and South), and canopy fractional cover also into two classes (open and forested). See Table 6 for a summary of snow depth with each class.

Category	LIDAR Snow Depth
High - North - Open	0.27
High - North - Forest	0.67
High - South - Open	0.25
High - South - Forest	0.64
Medium - North - Open	0.36
Medium - North - Forest	0.26
Medium - South - Open	0.26
Medium - South - Forest	0.2
Low - North - Open	0.19
Low - North - Forest	0.14
Low - South - Open	0.13
Low - South - Forest	0.11

Table 6. Mean snow depth for reclassified GIS model

Elevation was the primary stratification in the model due to strong literature support of the orographic effect (Anderton *et al.*, 1994; Pomeroy and Gray, 1995), and field and LiDAR observations of increasing snow depth with elevation. Slope was not included in the GIS model due to the errors associated with steeper slopes (Baltsavias, 1999; Butler, 2005; Deems and Painter, 2006; Hodgson *et al.*, 2005; Hollaus *et al.*, 2006) and our observations of high snow depth variance with increasing slope (Figure 18).

Given the variations in snow depth with aspect and canopy cover were generally small in both the field and LiDAR observation, it was decided to apply a binary stratification of the extremes for each class. To ascertain whether or not a significant difference existed in snow depth between north and south facing slopes or between open and forest covered areas, t-Tests were performed. In both cases, snow depths were significantly different at the 95%

level of confidence with a similar magnitude of stratification for each; i.e. neither canopy cover nor aspect could be said to have a strongly dominant role.

Lessons learned from the single terrain variable elevation led to the reprocessing of the GIS model using different elevation classes. The second evaluation of elevation led to a new classification. Elevation was classed into Low (1200 – 1700m), Medium (1700 – 2200) and High (2200 – 3200m). This classification takes into consideration the elevation of the tree line, therefore anything above the tree line is classified as high.

The steps required to create this model were as follows:

A) The LiDAR DEM was classed into low, medium and high elevations: Low (1200 – 1700m), Medium (1700 – 2200) and High (2200 – 3200m). Aspect was re-classed into north and south (270 – 90°, 90 - 270°) and fractional cover was re-classed into open and forested (0 - 30%, greater than 30%).

B) Each of the seven classes defined above were separated into their own raster layer using the “extract by attribute” in spatial analyst.

C) The seven rasters were converted to polygons using the “polygon to raster” tool under conversion tools.

D) Using the intersect tool, twelve unique classes were created using the combination of elevation, aspect and fractional cover. (E.g. High-South-Forest, High-South-Open, etc.)

E) Twelve snow depth rasters are created by using the above polygons as a mask to extract (extract by mask) snow depth values from the LiDAR snow depth dataset.

F) LiDAR snow depth averages were extracted for each of the unique twelve raster classes.

G) Steps A-E were repeated to create the same files for the Elbow River watershed using the SRTM and AVI datasets.

H) The snow depth averages calculated in step ‘F’ were applied to the watershed classes derived from the SRTM and AVI datasets.

Applying LiDAR-derived class-based snow depth averages to the extracted Elbow SRTM and AVI watershed attributes resulted in a snow water equivalent of 42,582,562m³ (Table 7). Visual representations of snow depth with the predictive values applied are shown in Figure 24. This estimated a snow water equivalent within 10,000m³ of the estimate calculated from elevation alone (when a drop in snow depth above the tree line is factored in). This demonstrates that terrain attributes such as aspect, and fractional cover are much weaker predictors than elevation and, as long as the elevation model is accurate (i.e. accounts for tree line effects), then this may be the only watershed attribute needed for a reasonable first approximation of watershed snow volume.

Snow Water Equivalent Calculated By Reclassed GIS Model							
Catagory	LIDAR Snow Depth	Cell Count (Watershed)	Cell Size	Area	Volume Snow (m ³)	SWE	
High - North - Open	0.27	10659	8100	86337900	23311233		
High - North - Forest	0.67	441	8100	3572100	2393307		
High - South - Open	0.25	11014	8100	89213400	22303350		
High - South - Forest	0.64	486	8100	3936600	2519424		
Medium - North - Open	0.36	7790	8100	63099000	22715640		
Medium - North - Forest	0.26	16082	8100	130264200	33868692		
Medium - South - Open	0.26	8142	8100	65950200	17147052		
Medium - South - Forest	0.2	14227	8100	115238700	23047740		
Low - North - Open	0.19	3543	8100	28698300	5452677		
Low - North - Forest	0.14	11933	8100	96657300	13532022		
Low - South - Open	0.13	3160	8100	25596000	3327480		
Low - South - Forest	0.11	8764	8100	70988400	7808724		
Total Volume					177427341	42582562	0.24

Table 7. Snow water equivalent calculated by re-classed GIS model

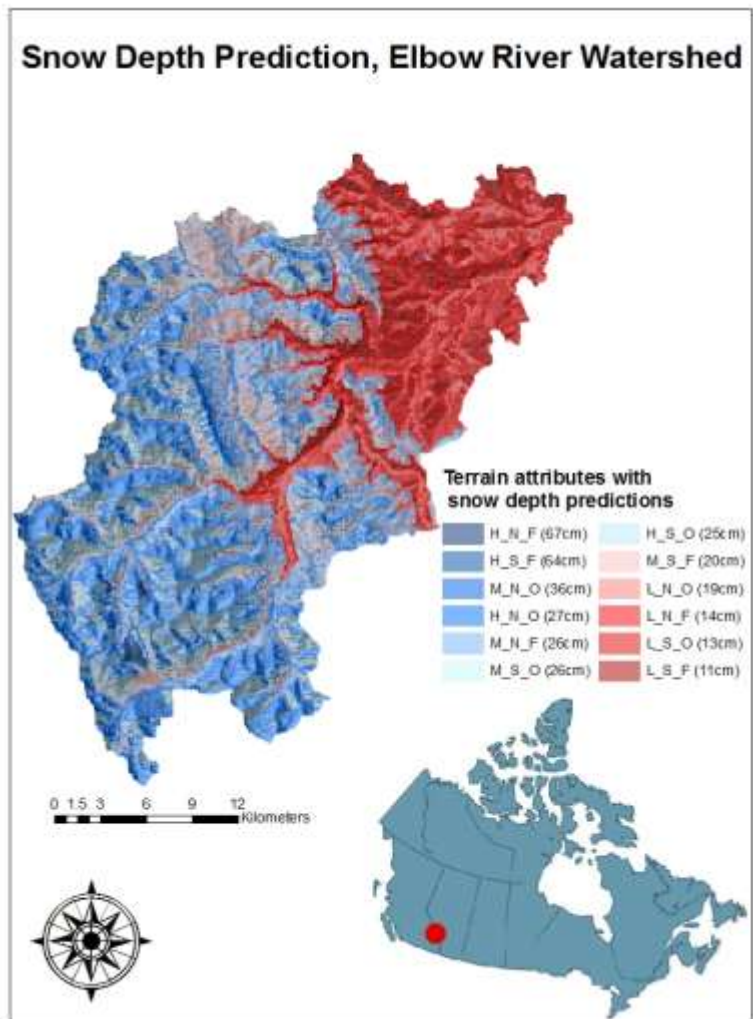


Figure 24. LiDAR-based GIS snow depth model applied to Elbow River watershed

Discussion and Conclusions

The mean snow depth from all 1675 field measurements equaled 0.28m with a standard deviation of 0.27m. The LiDAR derived mean snow depth equaled 0.18m with a standard deviation of 1.6m but after filtering the data for depths exceeding 5cm (noise level), the average became 0.26m; much closer to the field estimates which were collected only in snow covered areas. The high standard deviation in the LiDAR data illustrates the effects both of uncertainty (error) in the data plus a wide range of snow depths throughout the study area.

Elbow watershed SWE estimates range from $34.5 \times 10^6 \text{m}^3$ to $46.9 \times 10^6 \text{m}^3$. The highest estimates are based on a linear extrapolation of the observed elevation trend within the LiDAR data collected on the northern side of the Elbow Watershed. The actual watershed has a greater elevation range than sampled by the Elbow LiDAR dataset and so linear extrapolation of the LiDAR results may not be appropriate. Indeed, in the Marmot LiDAR observations (Figure 14), there was a clear peak in snowpack depth at tree line with depths leveling off or reducing above this elevation (approx 2200m a.s.l). Therefore, linearly extrapolating snowpack depth with height probably leads to an overestimate of snowpack depth. The modified class-based GIS model for Elbow snow volume accounts for the drop off in snow depth observed above tree line in the Marmot LiDAR data and generates a SWE estimate that lies near the middle of the range $42.6 \times 10^6 \text{m}^3$.

While the LiDAR and field snow depth data appear to be comparable and the watershed SWE estimates all within 25% of one another, some consideration of the errors and uncertainties inherent in this type of analysis is warranted.

LiDAR derived DEMs contain inherent position and elevation uncertainties related to: a) sensor system limitations; b) land cover induced error; and c) terrain error propagation. System error refers to the errors that can propagate from the individual components of the LiDAR sensor. The components of an airborne LiDAR system include the Global Positioning Unit (GPS), the inertial motion unit (IMU), Laser Ranging System, and the Scanning Mirror Unit (Baltsavias, 1999; Katzenbeisser, 2003; Wehr and Lohr, 1999). These systems have to be working together accurately and precisely in order to achieve high-accuracy data. For the altitudes flown over Marmot and Elbow, assuming all components are working correctly, the GPS quality is high and the sensor is appropriately calibrated, the expected uncertainties over hard unambiguous surfaces (such as highways and buildings) are approx. 15cm (RMSE) in the vertical and 50cm horizontal (Optech, ALTM 3100 specifications).

Landcover attributes can introduce errors that are in addition to the expected instrument precision (ASPRS Guidelines, 2004; Butler, 2005; Deems and Painter, 2006; Hodgson *et al.*, 2005; Hopkinson *et al.*, 2005; Hollaus *et al.*, 2006). Surface attributes such as roughness, reflectivity and vegetation cover can affect the vertical accuracy. A study

performed in North Carolina studied the effects of scrub-shrub, high grass, short grass, pavement, and various tree canopies on the returns acquired by LIDAR systems (Hodgson *et al.*, 2005). The study found that scrub-shrub returned the most vertical error (0.26m), followed by pine trees (0.24m), deciduous and mixed forest (0.20m) (leaf-off), and pavement (0.20m). High grass (0.12m) and short grass (0.11m) showed the least amount of vertical error. In a similar study by Hopkinson *et al.* (2005), they reported errors of 0.29m for aquatic vegetation, 0.04m for grass, 0.39m for low shrubs, and 1.09m for tall shrubs. In tree stands the LiDAR pulse reflects off the different levels of vegetation on the way through the canopy layer (Hodgson *et al.*, 2005; Hollaus *et al.*, 2006; Hopkinson *et al.*, 2005).

A further influence on the vertical error is the slope of the terrain (Baltsavias, 1999; Butler, 2005; Deems and Painter, 2006; Hodgson *et al.*, 2005; Hollaus *et al.*, 2006). Slopes cause the laser pulse to spread out over a larger footprint (Figure 25). The larger laser footprint increases the pulse response time at the sensor, called “time-walk” (Deems and Painter, 2006). Butler (2005) illustrated that as slope increases so does the vertical error. For a relatively steep slope (10-30 degrees) the elevation error can increase from 0.15m RMSE to 0.25m RMSE for a 1m grid. Vertical error is also affected by resolution: if the grid size is increased to a 2m grid the vertical error associated with the same slope was evaluated at 0.63m RMSE (Butler, 2005). Hollaus *et al.* (2005) also found that errors increased with slope. It was found that DTM errors increase from 10cm for relatively flat terrain (<10°) to over 50cm for local slopes greater than 60°.

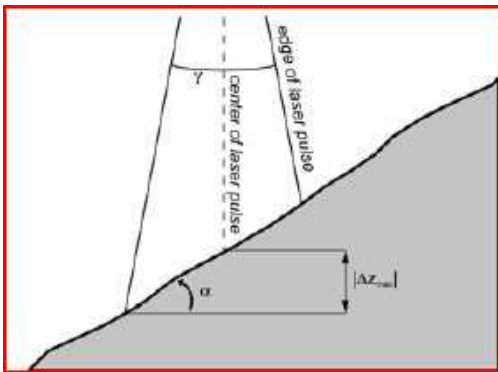


Figure 25: Example of how slope affects vertical accuracy (Deems and Painter, 2006)

Horizontal error and vertical error are interrelated. DEM errors most frequently occur in areas of steep terrain where the slightest horizontal shift will introduce an additional vertical error (ASPRS Guidelines, 2004; Butler, 2005; Hodgson *et al.*, 2005). Figure 26 illustrates how a small horizontal error can lead to a vertical error on a steep slope. If the x or y value for the location of the return registers to be left or right of the true location, then this places the point further up or down the slope of the true position, thereby introducing vertical error.

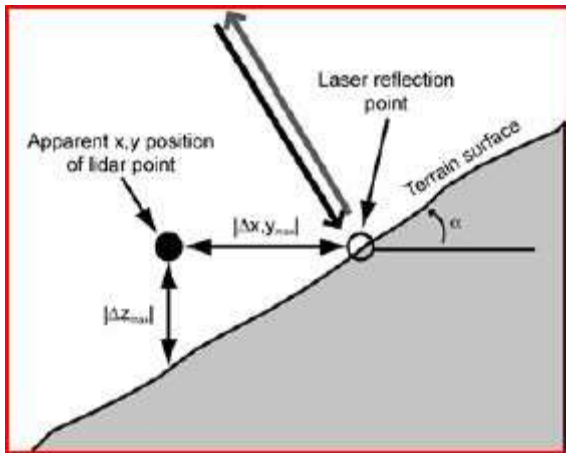


Figure 16: Inter-relation of horizontal and vertical error due to slope (Deems and Painter, 2006)

From the discussion above, it is clear that the alpine terrain and vegetated land covers within the Elbow and Marmot Creek study areas are likely to introduce a margin of uncertainty into each of the DEMs used for the snow depth analysis. Based on the results of the studies discussed, these uncertainties are expected to fall in the range of 10cm (flat terrain with no vegetation) up to a metre or more in steep or very densely vegetated areas. This error will be further magnified during the DEM subtraction routine to generate maps of snow depth. Hopkinson and Demuth (2006) noted several metres of negative surface error around cliff edges when applying a similar technique over the Peyto Glacier basin, also in the Canadian Rockies. These errors were the result of slight (sub 1m) horizontal offsets in one of the DEMs and they illustrate that any DEM change surface (e.g. snow depth) will be unreliable in the steepest part of the DEM.

Likely errors in the LiDAR snow depth estimates made in this study are apparent in the deep and highly variable estimates present in the steep slope classes in Figures 13 and 18. Fortunately, while such errors can be high in magnitude, they will tend to be random at the large scale, such that positive and negative errors may compensate one another. Further, steep slopes (over 60%) account for a small proportion of the overall area (less than 10%), while cliff faces by their vertical nature account for very little of planar surface area within the DEMs. Any elevation and subsequent depth errors along cliff edges, while they may be high, will be manifest over very small areas and thus not contribute greatly to overall snow volume estimates. In future analyses, these types of errors could potentially be mitigated by masking out cliff edges so that they do not bias the LiDAR based estimate of snow depth.

Further, it was found that in the case of both Marmot and Elbow, small block adjustments or translations of up to 50cm in one of the DEMs were necessary in order to align them (Figure 4). This was a challenging process in the heterogeneous and canopy covered parts of the study areas so the alignments relied on highway and building features that were found in the lower reaches of both datasets. Thus, it is possible that some residual misalignment and therefore snowpack depth error remains in the higher and more remote areas of the study areas. This could potentially be mitigated in the future if 3D

targets of rectilinear shape and several metres in dimension were erected in the more remote regions with the express purpose of assisting the LiDAR DEM alignment and co-registration process.

Our LiDAR-based estimate of SWE for the Elbow watershed above Bragg Creek is $40 \times 10^6 \text{m}^3 \pm 10 \times 10^6 \text{m}^3$. However, due to the many uncertainties discussed above, the true value may deviate significantly from this estimated range. At the time of the LiDAR and field data collections, snow conditions were abnormally depleted relative to most years and this greatly limited what could be achieved with this experiment. The observed snowpack depths at both study sites (particularly Elbow) were close to the practical detection limit given expected LiDAR DEM uncertainties. With observed average snow depths in Elbow below 30cm it is actually quite encouraging that the LiDAR estimates were very close. More reliable results would no doubt be achieved if the snowpack were deeper but without co-registered LiDAR and field data it is impossible to accurately determine what the lowest viable average snow depth would be. We are convinced that it is above the depths observed in this study, as in almost all cases, the standard deviation of depth uncertainty was close to the mean; i.e. 100% uncertainty! For a practical application of this method, the uncertainty would have to be reduced to an acceptable level. If 25% uncertainty limits are considered acceptable, then this implies that average watershed depths would need to approach 1m. In many years, such conditions probably do occur in the upper reaches of the Elbow and almost certainly for other watersheds further west.

A logistical setback to the study was our inability to perform direct comparisons of field to LiDAR snow depth data due to the LiDAR survey lines not following the planned flight paths. In order to perform a more thorough sensitivity analysis of this method, the experiment could be performed again over an area of deeper snowpack with absolutely co-located field and lidar data. More work is also needed to validate the watershed estimate of SWE. This could involve running a hydrological model on the Elbow Creek during spring runoff and comparing to the flow records to see if the antecedent snowpack conditions derived by LiDAR leads to an accurate simulation of runoff magnitude.

Acknowledgements

Sustainable Resources Development (SRD) and City of Calgary are acknowledged for funding and supporting the project. SRD and Alberta Environmental Protection (AEP) also provided field equipment and logistical support in the form of helicopter time and ATVs. Dr John Pomeroy and students from University of Saskatchewan are acknowledged for providing field accommodation and assisting with data collection over Marmot Creek watershed. Dr Pomeroy and the IP3 research network are acknowledged for paying most of the acquisition costs associated with the 2007 LiDAR data acquisition over Marmot Creek. Wolf Survey is thanked for loaning the AGRG crew a truck, ATV and several items of field survey equipment. Airborne Imaging is gratefully acknowledged for flying the 2008 LiDAR data collections and processing the basic outputs at a heavily subsidized rate below the normal commercial price. James Churchill and Tim Collins are gratefully acknowledged for their hard work and diligence during long days in the field.



Photo of AGRG field crew whilst undertaking field snow depth sampling in the Elbow. Left to Right: Tim Collins, Chris Hopkinson, James Churchill.

LiDAR and snowpack bibliography:

- Adams, W. and Barr, D., 1979. Vegetation-snow relationships in Labrador. *Proc. of the Eastern Snow Conference, 36th Annual Meeting*. Alexandria Bay, New York.
- Alberta Environmental Protection, 2000, *Snow Survey Report for the Bow River Basin, Alberta, Canada*. Provided by Dick Allison, formerly of Alberta Environmental Protection.
- ALTM 3100 EA specifications. Optech Inc., Retrieved on October 22, 2008. http://www.optech.ca/pdf/Specs/specs_altm_3100.pdf
- Anderton, S.P., White, S.M., & Alvera, B. 2004. *Evaluation of spatial variability in snow water equivalent for a high mountain catchment*. *Hydrological Processes*, 18, 435-453.
- ASPRS Guidelines. *Vertical Accuracy Reporting for LIDAR data*. May24, 2004.
- Baltsavias, E.P. 1999. *Airborne laser scanning: basic relations and formulas*. *ISPRS Journal of Photogrammetry and Remote Sensing*, 54, 199-214.
- Baltsavias, E.P. 1999. *Airborne laser scanning: Existing systems and firms and other resources*. *ISPRS Journal of Photogrammetry and Remote Sensing*, 54, 164-198.
- Baltsavias, E.P., 1999. *Airborne laser scanning: basic relations and formulas*. *ISPRS Journal of Photogrammetry and Remote Sensing*, 54: 199-214.
- Borneuf, D. 1980. *Hydrogeology of the Kananaskis Lake Area, Alberta*. Alberta Research Council, Earth Sciences Report 79-4, 1-16.
- Bréda, N.J.J. 2003. *Ground-based measurements of Leaf-area index: a review of methods, instruments and current controversies*. *Journal of Experimental Botany*, 54, 2403 – 2417.
- BSc Environmental Science. 2002. *Water Quality Impacts by Private Sewage Disposal Systems (PSDSs) in Bragg Creek, Alberta: Current Assessment and Residents Views*. BSc. Environmental Science Program, University of Calgary. 160pp.
- Bulter, D.S. 2005. *An evaluation of LIDAR terrain data in the context of varying topography*. Masters Thesis submitted.
- Chasmer, L. and Hopkinson, C., 2001. Using airborne laser altimetry and GIS to assess scale induced radiation-loading errors in a glacierised basin. *Proc. of the 58th Eastern Snow Conference*. Ottawa, Ontario, Canada. May 14 – 18, 2001.
- Collins, J.P., Langley, R.B. 1996. *Mitigating tropospheric propagation delay errors in precise airborne GPS navigation*. Position Location and Navigational Symposium.

- Corsini, A., Borgatti, L., Coren, F., & Vellico, M. 2007. *Use of Multi-temporal airborne LIDAR surveys to analyse post-failure of earth slides*. Canadian Journal of Remote Sensing, 33, 116-120.
- Deems, J.S., and Painter, T.H. 2006. *Lidar measurement of snow depth: Accuracy and error sources*. Proceedings of the 2006 International Snow Science Workshop, Telluride, CO, 384-391.
- Deems, J.S., Fassnacht, S.R., Elder, K.J. 2006. *Fractal distribution of snow depth from LiDAR data*. Journal of Hydrometeorology 7, 285 - 297.
- Derksen, C., LeDrew, E., Walker, A. and Goodison, B, 2001. Evaluation of the Meteorological Service of Canada Boreal Forest snow water equivalent algorithm. *Proc. of the 58th Eastern Snow Conference*. Ottawa, Ontario, Canada. May 14 – 18, 2001.
- Elder, K., Rosenthal, W., and Davis, R., 1998. Estimating the spatial distribution of snow water equivalence in a montane watershed. *Hydrological Processes*, 12:1793-1808.
- Environment Canada. Retrieved on October 14th, 2008. <http://www.climate.weatheroffice.ec.gc.ca/>
- Essery, R., Li, L., Pomeroy, J. 1999. *A distributed model of blowing snow over complex terrain*. Hydrological Processes, 13, 2423-2438.
- Fassnacht, S.R., and Deems, J.S. 2005. *Scaling associated with averaging and resampling of LIDAR-derived mountane snow depth data*. 62nd Eastern Snow Conference, Waterloo ON, Canada.
- Flood, M., and Gutelius, B., 1997. Commercial implications of topographic terrain mapping using scanning airborne laser radar. *Photogramm. Eng. Rem. Sens.* 63: 327-366.
- Golden Software Inc. 1995. *Surfer[®] for Windows, version 6: user's guide*, Golden Software Inc. Colorado.
- Golden Software. *Gridding Overview*, accessed online <http://quake.unr.edu/ftp/pub/louie/class/333/contour/surfer.pdf> [Accessed on 7 November 2008]
- Goodison, B. E., Ferguson, H. L., and McKay, G. A., 1981. Measurement and data analysis, in *The Handbook of Snow; Principles, processes, management and use*, (ed. D.M. Gray and D. H. Male), Toronto: Pergamon Press, pp. 191-274.
- Goulden, T., and Hopkinson, C. 2008. *The Forward Propagation of System related errors with LIDAR data*. Hydroscan: Airborne laser mapping of hydrological features and resources, 47-68.
- Gutelius, W., 1998. Engineering Applications of Airborne Scanning Lasers: Reports From the Field. *Photogramm. Eng. Rem. Sens.* 64, 246-253.
- Hedstrom, N.R., Pomeroy, J.M. 1998. *Measuring and modelling of snow interception in the boreal forest*. Hydrological Processes, 12, 1611-1625.

- Heimstra, C.A., Liston, G.E., Reiners, W.A. 2002. *Snow Redistribution by Wind Interactions with Vegetation at Upper Treeline in the Medicine Bow Mountains, Wyoming, U.S.A.* Arctic, Antarctic, and Alpine Research, 34, 262 – 273.
- Hodgson, M.E., Jensen, J., Raber, G., Tullis, J., Davis, B.A., Thompson, G., & Schuckman, K. 2005. *An evaluation of LIDAR-derived elevation and terrain slope in leaf-off conditions.* Photogrammetric Engineering and Remote Sensing, 71, 817-823.
- Holden, N., 1998. *Airborne LiDAR feasibility study*, United Kingdom Environment Agency Research and Development technical report no. TR E43
- Hollaus, M., Wagner, W., Eberhöfer, C., & Karel, W. 2006. *Accuracy of large scale canopy heights derived from LIDAR data under operational constraints in a complex alpine environment.* ISPRS Journal of Photogrammetry and Remote Sensing, 60, 323-338.
- Hopkinson, C. and Chasmer, L. Hall, R. 2008. The uncertainty in conifer plantation growth prediction from multitemporal lidar datasets. *Remote Sensing of Environment.* Vol. 112, No.3.
- Hopkinson, C. Chasmer, L. 2009. *Testing LIDAR models of fractional cover across multiple forest ecozones.* Remote Sensing of Environment. (In Press).
- Hopkinson, C., Chasmer, L.E., Sass, G., Creed, I.F., Sitar, M., Kalbfleisch, W., Trietz, P. 2005. *Vegetation class dependant errors in lidar ground elevation and canopy height estimates in a boreal wetland environment.* Canadian Journal of Remote Sensing, 31, 191-206.
- Hopkinson, C., Demuth, M.N. 2006. "Using airborne lidar to assess the influence of glacier downwasting to water resources in the Canadian Rocky Mountains", *Canadian Journal of Remote Sensing*, 32 (2) pp. 212-222.
- Hopkinson, C., Demuth, M.N., Sitar, M. and Chasmer, L.E., 2001. Applications of Airborne LiDAR Mapping in Glacierised Mountainous Terrain. *Proc. of the International Geoscience and Remote Sensing Symposium.* Sydney, Australia, July 9-14, 2001.
- Hopkinson, C., Hayashi, M., Peddle, D. 2009. "Comparing alpine watershed attributes from LiDAR, Photogrammetric, and Contour-based Digital Elevation Models." *Hydrological Processes* (In Press).
- Hopkinson, C., Sitar, M., Chasmer, L.E., & Treitz, P. 2004. *Mapping snowpack depth beneath forest canopies using airborne LIDAR.* Photogrammetric Engineering and Remote Sensing, 70, 323-330.
- Hopkinson, C., Sitar, M., Chasmer, L.E., Treitz, P. 2004. "Mapping Snowpack Depth Beneath Forest Canopies Using Airborne LiDAR." *Photogrammetric Engineering and Remote Sensing*, 70 (3) pp. 323-330
- Katzenbeisser, R. 2003. *About the Calibration of Lidar Sensors*, ISPRS Workshop 3-D Reconstruction from Airborne Laser-Scanner and InSAR data, 8 -10 October.

- Kennet, M. and Eiken, T., 1997. Airborne measurement of glacier surface elevation by scanning laser altimeter. *Annals Glaciol.* 24, 235-238,
- Krabill, W.B., Thomas, Jezek, Kuivinen and Manizade, 1995. Greenland Ice Sheet Thickness Changes Measured by Laser Altimetry, *Geophys. Res. Letters*, 22, 2341-2344
- Latypov, D. 2005. *Effects of laser beam alignment tolerance on LIDAR accuracy*. ISPRS Journal of Photogrammetry and Remote Sensing, 59, 361-368.
- Lim, K., Treitz, P. Wulder, M. St-Onge, B. and Flood, M., 2003, LiDAR Remote Sensing of Forest Structure, *Prog. Phys. Geog.* 27: 88-106.
- Lim, K., Treitz, P., Groot, A., St-Onge, B., 2001. Estimation of individual tree heights using LiDAR remote sensing, *Proc. of the 23rd Canadian Symposium on Remote sensing*, Sainte-Foy Quebec, 251-258.
- Lopez-Moreno, J.I., Laton, J. 2008. *Influence of canopy density on snow distribution in a temperate mountain range*. Hydrological Processes, 22, 117-126.
- MacMicheal , G. (editor). 2000. *Bi-Weekly Bulletin*. Agriculture and Agri-Food Canada, Vol. 19, No.19.
- McKay, G. A. and Gray, D. M., 1981. The distribution of snowcover, in *The Handbook of Snow; Principles, processes, management and use*, (ed. D.M. Gray and D. H. Male), Toronto: Pergamon Press, 153-189.
- Means, J., Acker, S., Fitt, B., Renslow, M., Emerson, L., and Hendrix, C., 2000. Predicting forest stand characteristics with airborne scanning lidar. *Photogramm. Eng. Rem. Sens.* 66: 1367-1371.
- Mitchell, P., Prepas, E. 1990. *Atlas of Alberta Lakes*. University of Alberta Press, Edmonton, 564-569.
- Mote, T.C., & Grundstein, A.J. 2003. *A comparison of modeled, remotely sensed, and measured snow water equivalent in the Northern Great Plain*. Water Resources Research, 39, 1-12.
- Musselman, K.N., Molotch, N.P, & Brook, P.D. 2008. *Effects of vegetation on snow accumulation and ablation in a mid-latitude sub-alpine forest*. Hydrological Processes. Available from <www.interscience.wiley.com>. [Accessed 17 June 2008].
- National Snow and Ice Data Centre, Available from <http://nsidc.org/data/swe/> [Accessed 6 November 2008].
- Pomeroy, J.W., Gray, D.M. 1995. *Snowcover Relocation and Management*. NHRI Science Report 7, Saskatoon.
- Pomeroy, J.W., Gray, D.M., Hedstrom, N.R., & Janowicz, J.R. 2002. *Prediction of seasonal snow accumulation in cold climate forests*. Hydrological Processes, 16, 3543-3558.

- Reese, W.G., & Arnold, N.S. 2007. *Mass balance and dynamic of a glacier measured by high-resolution Lidar*. Polar Record, 43, 311-319.
- Sicart, J.E., Pomeroy, J.W., Essery R.L.H., Bewley, D. 2006. *Incoming longwave radiation to melting snow: observations, sensitivity and estimation in northern environments*. Hydrological Processes, 20, 3687-3708.
- St-Onge, B., Dufort, J., and Lepage, R., 2000. Measuring tree height using scanning laser altimetry. *Proc. of the 22nd Annual Canadian Remote Sensing Symposium*, Victoria, BC, Canada. August 21 – 25, 2000.
- Tao, C.V., & Hu, Y. 2002. *Assessment of airborne LIDAR and imaging technology for pipeline mapping and safety applications*. Pecora 15/Land Satellite Information IV/ISPRS Commission I/FIEOS 2002 Conference Proceedings.
- Wehr, A., & Lohr, U. 1999. *Airborne laser scanning – an introduction and overview*. ISPRS Journal of Photogrammetry and Remote Sensing, 54, 68-86.
- Wulder, M.A., Han, T., White, J.C., Sweda, T., & Tusuzuki, H. 2007. *Integrating profiling LIDAR with Landsat for regional boreal forest canopy attribute estimation and change characterization*. Remote Sensing of Environment, 110, 123-137.

Appendices

A.1. Individual Transect Summaries

Transect 1	
Aspect	West
Slope	22.5 -45.0
Elevation	1300 - 1400
Average Snow Depth	0.44
Fractional Cover A	0.24
Snow Depth @ A	0.61
Fractional Cover B	0.12
Snow Depth @ B	0.07
Open	0.44
Forested	N/A
standard deviation (o)	0.264
standard deviation (f)	N/A
t-test	N/A

Transect 2	
Aspect	West
Slope	22.5 - 45.0
Elevation	1400 - 1500
Average Snow Depth	0.22
Fractional Cover A	0.34
Snow Depth @ A	0.21
Fractional Cover B	N/A
Snow Depth @ B	
Open	0.22
Forested	N/A
standard deviation (o)	0.118
standard deviation (f)	N/A
t-test	N/A

Transect 3	
Aspect	West
Slope	22.5 - 45.00
Elevation	1400 - 1500
Average Snow Depth	0.15
Fractional Cover A	0.43
Snow Depth @ A	0.08
Fractional Cover B	0.11
Snow Depth @ B	0
Open	0.23
Forested	0.05
standard deviation (o)	0.096
standard deviation (f)	0.065
t-test	0.0003

Transect 4	
Aspect	flat
Slope	0 - 22.5
Elevation	1400 - 1500
Average Snow Depth	0.23
Fractional Cover A	0.7
Snow Depth @ A	0.18
Fractional Cover B	N/A
Snow Depth @ B	
Open	0.21
Forested	0.23
standard deviation (o)	0.02
standard deviation (f)	0.08
t-test	0.523

Transect 5	
Aspect	North
Slope	0 - 22.5
Elevation	1500 - 1600
Average Snow Depth	0.34
Fractional Cover A	0.2
Snow Depth @ A	0.39
Fractional Cover B	N/A
Snow Depth @ B	
Open	0.34
Forested	0.28
standard deviation (o)	0.26
standard deviation (f)	0.122
t-test	0.659

Transect 6	
Aspect	flat
Slope	0 - 22.5
Elevation	1500 - 1600
Average Snow Depth	0.27
Fractional Cover A	0.26
Snow Depth @ A	0.34
Fractional Cover B	N/A
Snow Depth @ B	
Open	0.31
Forested	0.22
standard deviation (o)	0.15
standard deviation (f)	0.17
t-test	0.388

Transect 7	
Aspect	South
Slope	0 - 22.5
Elevation	1500 - 1600
Average Snow Depth	0.33
Fractional Cover A	0.7
Snow Depth @ A	0.31
Fractional Cover B	N/A
Snow Depth @ B	
Open	0.4
Forested	0.33
standard deviation (o)	0.05
standard deviation (f)	0.03
t-test	1.394E-17

Transect 8	
Aspect	South
Slope	0 - 22.5
Elevation	1600 - 1700
Average Snow Depth	0.27
Fractional Cover A	0.1
Snow Depth @ A	0.35
Fractional Cover B	0.71
Snow Depth @ B	0.17
Open	0.17
Forested	0.38
standard deviation (o)	0.12
standard deviation (f)	0.11
t-test	0.0005

Transect 9	
Aspect	South
Slope	22.5 - 45.0
Elevation	1600 - 1700
Average Snow Depth	0.38
Fractional Cover A	0.74
Snow Depth @ A	0.52
Fractional Cover B	0.77
Snow Depth @ B	0.24
Open	0.46
Forested	0.36
standard deviation (o)	0.32
standard deviation (f)	0.18
t-test	0.456

Transect 11	
Aspect	East
Slope	0 - 22.5
Elevation	1500 - 1600
Average Snow Depth	0.15
Fractional Cover A	0.68
Snow Depth @ A	0.11
Fractional Cover B	0.36
Snow Depth @ B	0.6
Open	0.2
Forested	0.11
standard deviation (o)	0.17
standard deviation (f)	0.12
t-test	0.081

Transect 12	
Aspect	West
Slope	0 - 22.5
Elevation	1600 - 1700
Average Snow Depth	0.27
Fractional Cover A	0.11
Snow Depth @ A	0.26
Fractional Cover B	0.36
Snow Depth @ B	0.53
Open	0.26
Forested	0.35
standard deviation (o)	0.08
standard deviation (f)	0.19
t-test	0.221

Transect 13	
Aspect	flat
Slope	0 - 22.5
Elevation	1800 - 1900
Average Snow Depth	0.18
Fractional Cover A	0.74
Snow Depth @ A	0.35
Fractional Cover B	0.05
Snow Depth @ B	0.26
Open	0.2
Forested	0.16
standard deviation (o)	0.12
standard deviation (f)	0.12
t-test	0.491

Transect 14	
Aspect	North
Slope	0 - 22.5
Elevation	1700 - 1800
Average Snow Depth	0.48
Fractional Cover A	0.56
Snow Depth @ A	0.52
Fractional Cover B	0.41
Snow Depth @ B	0.5
Open	0.49
Forested	N/A
standard deviation (o)	0.11
standard deviation (f)	N/A
t-test	N/A

Transect 15	
Aspect	East
Slope	0 - 22.5
Elevation	1600 - 1700
Average Snow Depth	0.19
Fractional Cover A	0.58
Snow Depth @ A	0.21
Fractional Cover B	0.05
Snow Depth @ B	0.18
Open	0.2
Forested	0.13
standard deviation (o)	0.18
standard deviation (f)	0.16
t-test	0.520

Transect 16	
Aspect	West
Slope	0 - 22.5
Elevation	1800 - 1900
Average Snow Depth	0.29
Fractional Cover A	0.72
Snow Depth @ A	0.35
Fractional Cover B	0.65
Snow Depth @ B	0.4
Open	0.32
Forested	0.25
standard deviation (o)	0.18
standard deviation (f)	0.10
t-test	0.321

Transect 23	
Aspect	East
Slope	0 - 22.5
Elevation	1600 - 1700
Average Snow Depth	0.37
Fractional Cover A	0.06
Snow Depth @ A	0.18
Fractional Cover B	0.7
Snow Depth @ B	0.27
Open	0.48
Forested	0.24
standard deviation (o)	0.17
standard deviation (f)	0.03
t-test	0.012

Transect Elbow	
Aspect	North
Slope	0 - 22.5
Elevation	NA
Average Snow Depth	0.16
Fractional Cover A	0.7
Snow Depth @ A	0.25
Fractional Cover B	0.84
Snow Depth @ B	0.01
Open	0.26
Forested	0.11
standard deviation (o)	0.11
standard deviation (f)	0.09
t-test	0.113

Transect Quirk	
Aspect	East
Slope	0 - 22.5
Elevation	1600 - 1700
Average Snow Depth	0.12
Fractional Cover A	0.24
Snow Depth @ A	0.15
Fractional Cover B	0.06
Snow Depth @ B	0
Open	0.12
Forested	N/A
standard deviation (o)	0.09
standard deviation (f)	N/A
t-test	N/A

Transect Sylvester	
Aspect	North
Slope	0 - 22.5
Elevation	1500 - 1600
Average Snow Depth	0.25
Fractional Cover A	0.02
Snow Depth @ A	0.33
Fractional Cover B	0.08
Snow Depth @ B	0.22
Open	0.25
Forested	N/A
standard deviation (o)	0.12
standard deviation (f)	N/A
t-test	N/A

Transect Valley	
Aspect	North
Slope	0 - 22.5
Elevation	N/A
Average Snow Depth	0.27
Fractional Cover A	0.63
Snow Depth @ A	0
Fractional Cover B	0.64
Snow Depth @ B	0.21
Open	0.34
Forested	0.12
standard deviation (o)	0.19
standard deviation (f)	0.14
t-test	0.108

Transect 40	
Aspect	
Slope	
Elevation	2200 - 2300
Average Snow Depth	2.22
Fractional Cover A	
Snow Depth @ A	
Fractional Cover B	
Snow Depth @ B	
Open	2.22
Forested	N/A
standard deviation (o)	0.49
standard deviation (f)	N/A
t-test	N/A

Transect 41	
Aspect	
Slope	
Elevation	2100 - 2200
Average Snow Depth	0.71
Fractional Cover A	N/A
Fractional Cover B	N/A
Open	0.64
Forested	0.78
standard deviation (o)	0.42
standard deviation (f)	0.11
t-test	0.447

A.2. AVI Crown Closure comparison to DHP canopy fractional cover

DHP Location	Crown Closure	DHP Fractional Cover
1A	A	B
1B	A	B
2A	A	C
3A	C	C
3B	A	B
4A	D	D
5A	D	B
6A	A	B
7A	E	E
8A	A	B
8B	A	D
9A	C	D
9B	A	D
11A	C	D
11B	A	C
12A	A	B
12B	A	C
13A	E	E
13B	A	A
14A	D	D
14B	B	C
15A	A	A
16A	C	E
16B	C	D
23B	E	E
QuirkB	C	B
SYLV B	C	A

Exact Representation	30%
Within 1 Class range	44%

0 - 5%	A
6 - 30%	B
31 - 50%	C
51 - 70%	D
71 - 100%	E